UNIVERSIDAD DE CONCEPCIÓN

Centro de Investigación en Ingeniería Matemática (CI^{2}MA)

A posteriori error analysis for a sedimentation-consolidation system

Mario Álvarez, Gabriel N. Gatica,
Ricardo Ruiz-Baier

PREPRINT 2016-26

SERIE DE PRE-PUBLICACIONES

A posteriori error analysis for a sedimentation-consolidation system*

Mario Alvarez† Gabriel N. Gatica‡ Ricardo Ruiz-Baier§

Abstract

In this paper we develop the *a posteriori* error analysis of an augmented mixed–primal finite element method for the 2D and 3D versions of a stationary flow and transport coupled system, typically encountered in sedimentation-consolidation processes. The governing equations consist in the Brinkman problem with concentration-dependent viscosity, written in terms of Cauchy pseudo-stresses and bulk velocity of the mixture; coupled with a nonlinear advection – nonlinear diffusion equation describing the transport of the solids volume fraction. The solvability of the continuous mixed–primal formulation along with *a priori* error estimates for a finite element scheme using Raviart-Thomas spaces of order k for the stress approximation, and continuous piecewise polynomials of degree $\leq k+1$ for both velocity and concentration, have been recently established in [M. Alvarez et al., M3AS: Math. Models Methods Appl. Sci. 26 (5) (2016) 867–900]. In this work we derive two efficient and reliable residual-based *a posteriori* error estimators for that scheme. For the first estimator we make use of suitable ellipticity and inf-sup conditions together with a Helmholtz decomposition and the local approximation properties of the Clément interpolant and Raviart-Thomas operator to show its reliability, whereas the efficiency follows from inverse inequalities and localization arguments based on triangle-bubble and edge-bubble functions. Next, we analyze an alternative error estimator, whose reliability can be proved without resorting to Helmholtz decompositions. Finally, we provide some numerical results confirming the reliability and efficiency of the estimators and illustrating the good performance of the associated adaptive algorithm for the augmented mixed-primal finite element method.

Key words: Brinkman-transport coupling, nonlinear advection-diffusion, augmented mixed–primal formulation, sedimentation-consolidation process, finite element methods, *a posteriori* error analysis

Mathematics subject classifications (2000): 65N30, 65N12, 76R05, 76D07, 65N15.

1 Introduction

We have recently analyzed in [3], the solvability of a strongly coupled flow and transport system typically encountered in continuum-based models of sedimentation-consolidation processes. More

*This work was partially supported by CONICYT-Chile through BASAL project CMM, Universidad de Chile, and project Anillo ACT1118 (ANANUM); by the Ministery of Education through the project REDOC.CTA of the Graduate School, Universidad de Concepción; and by Centro de Investigación en Ingeniería Matemática (CI^{2}MA), Universidad de Concepción.

†Sección de Matemática, Sede de Occidente, Universidad de Costa Rica, San Ramón de Alajuela, Costa Rica, email: mario.alvarezguadamuz@ucr.ac.cr. Present address: CI^{2}MA and Departamento de Ingeniería Matemática, Universidad de Concepción, Casilla 160-C, Concepción, Chile, email: mguadamuz@ci2ma.udec.cl.

‡CI^{2}MA and Departamento de Ingeniería Matemática, Universidad de Concepción, Casilla 160-C, Concepción, Chile, email: ggatica@ci2ma.udec.cl.

§Mathematical Institute, Oxford University, Andrew Wiles Building, Woodstock Road, Oxford OX2 6GG, UK, email: ruizbaier@maths.ox.ac.uk.

precisely, the steady-state regime of a solid-liquid suspension immersed in a viscous fluid within a permeable medium is considered in [3], and the governing equations consist in the Brinkman problem with variable viscosity coupled with a nonlinear advection – nonlinear diffusion equation describing the transport model. An augmented variational formulation is then proposed there with main unknowns given by the Cauchy pseudo-stress and bulk velocity of the mixture, and the solids volume fraction, which are sought in $\mathbb{H}(\mathbf{div};\Omega)$, $\mathbf{H}^1(\Omega)$, and $\mathrm{H}^1(\Omega)$, respectively. Fixed point arguments, certain regularity assumptions, and some classical results concerning variational problems and Sobolev spaces are combined to establish the solvability of the continuous and discrete coupled formulations. Consequently, the rows of the Cauchy stress tensor were approximated with Raviart-Thomas elements of order k, whereas the velocity and solids concentration were discretized with continuous piecewise polynomials of degree $\leq k+1$. Suitable Strang-type estimates are employed to derive optimal *a priori* error estimates for the Galerkin solution.

The purpose of this work is to provide reliable and efficient residual-based *a posteriori* error estimators for the steady sedimentation-consolidation system studied in [3]. Estimators of this kind are frequently employed to guide adaptive mesh refinement in order to guarantee an adequate convergence behavior of the Galerkin approximations, even under the eventual presence of singularities. The global estimator $\boldsymbol{\eta}$ depends on local estimators η_T defined on each element T of a given mesh $\mathcal{T}_h$. Then, $\boldsymbol{\eta}$ is said to be efficient (resp. reliable) if there exists a constant $C_{\mathtt{eff}} > 0$ (resp. $C_{\mathtt{rel}} > 0$), independent of meshsizes, such that

$$C_{\mathtt{eff}}\,\boldsymbol{\eta} \,+\, \text{h.o.t.} \leq \|error\| \leq C_{\mathtt{rel}}\,\boldsymbol{\eta} \,+\, \text{h.o.t.}\,,$$

where h.o.t. is a generic expression denoting one or several terms of higher order. Up to the authors knowledge, a number of *a posteriori* error estimators specifically targeted for non-viscous flow (e.g, Darcy) with transport problems are available in the literature [7, 15, 26, 32, 35]. However, only [8, 27] and [4] are devoted to the *a posteriori* error analysis for coupled viscous flow-transport problems. In particular, we derive in [4], two efficient and reliable residual-based *a posteriori* error estimators for an augmented mixed–primal finite element approximation of a stationary viscous flow and transport problem, which serves as a prototype model for sedimentation-consolidation processes and other phenomena where the transport of species concentration within a viscous fluid is of interest.

In this paper, as well as in [4], we make use of ellipticity and inf-sup conditions together with a Helmholtz decomposition, local approximation properties of the Clément interpolant and Raviart-Thomas operator, and known estimates from [6], [17], [21], [23] and [24], to prove the reliability of a residual-based estimator. Then, inverse inequalities, the localization technique based on triangle-bubble and edge-bubble functions imply the efficiency of the estimator. Alternatively, we deduce a second reliable and efficient residual-based *a posteriori* error estimator, where the Helmholtz decomposition is not employed in the corresponding proof of reliability. The rest of this paper is organized as follows. In Section 2, we first recall from [3] the model problem and a corresponding augmented mixed-primal formulation as well as the associated Galerkin scheme. In Section 3, we derive a reliable and efficient residual-based *a posteriori* error estimator for our Galerkin scheme. A second estimator is introduced and analyzed in Section 4. Next, the analysis and results from Section 3 and 4 are extend to the three-dimensional case in Section 5. Finally, in Section 6, our theoretical results are illustrated via some numerical examples, highlighting also the good performance of the scheme and properties of the proposed error indicators.

2 The sedimentation-consolidation system

Let us denote by $\Omega \subseteq \mathrm{R}^n$, $n = 2, 3$ a given bounded domain with polyhedral boundary $\Gamma = \bar{\Gamma}_{\mathrm{D}} \cup \bar{\Gamma}_{\mathrm{N}}$, with $\Gamma_{\mathrm{D}} \cap \Gamma_{\mathrm{N}} = \emptyset$ and $|\Gamma_{\mathrm{D}}|$, $|\Gamma_{\mathrm{N}}| > 0$, and denote by $\boldsymbol{\nu}$ the outward unit normal vector on Γ. Standard

notation will be adopted for Lebesgue spaces $\mathrm{L}^p(\Omega)$ and Sobolev spaces $\mathrm{H}^s(\Omega)$ with norm $\|\cdot\|_{s,\Omega}$ and seminorm $|\cdot|_{s,\Omega}$. In particular, $\mathrm{H}^{1/2}(\Gamma)$ is the space of traces of functions of $\mathrm{H}^1(\Omega)$ and $\mathrm{H}^{-1/2}(\Gamma)$ denotes its dual. By $\mathbf{M}, \mathbb{M}$ we will denote the corresponding vectorial and tensorial counterparts of the generic scalar functional space M. We recall that the space

$$\mathbb{H}(\mathbf{div};\Omega) := \{\boldsymbol{\tau} \in \mathbb{L}^2(\Omega) : \quad \mathbf{div}\,\boldsymbol{\tau} \in \mathbf{L}^2(\Omega)\},$$

equipped with the usual norm

$$\|\boldsymbol{\tau}\|^2_{\mathbf{div};\Omega} := \|\boldsymbol{\tau}\|^2_{0,\Omega} + \|\mathbf{div}\,\boldsymbol{\tau}\|^2_{0,\Omega}$$

is a Hilbert space. As usual, $\mathbb{I}$ stands for the identity tensor in $\mathrm{R}^{n\times n}$, and $|\cdot|$ denotes both the Euclidean norm in R^n and the Frobenius norm in $\mathrm{R}^{n\times n}$.

2.1 The governing equations

The following model describes the steady state of the sedimentation-consolidation process consisting on the transport and suspension of a solid phase into an immiscible fluid contained in a vessel Ω (*cf.* [3]). The flow patterns are influenced by gravity and by the local fluctuations of the solids volume fraction. After elimination of the fluid pressure (cf. [3]), the process is governed by the following system of partial differential equations:

$$\begin{aligned} &\frac{1}{\mu(\phi)}\boldsymbol{\sigma}^{\mathtt{d}} = \nabla \boldsymbol{u}\,, \quad \boldsymbol{K}^{-1}\boldsymbol{u} - \mathbf{div}\,\boldsymbol{\sigma} = \boldsymbol{f}\phi\,, \quad \mathrm{div}\;\boldsymbol{u} = 0 \qquad \text{in} \quad \Omega\,, \\ &\widetilde{\boldsymbol{\sigma}} = \vartheta(\phi)\,\nabla\phi - \phi\boldsymbol{u} - f_{\mathrm{bk}}(\phi)\boldsymbol{k}\,, \quad \beta\,\phi - \mathrm{div}\;\widetilde{\boldsymbol{\sigma}} = g \qquad \text{in} \quad \Omega\,, \end{aligned} \tag{2.1}$$

along with the following boundary conditions:

$$\begin{aligned} &\boldsymbol{u} = \boldsymbol{u}_{\mathrm{D}} \quad \text{on} \quad \Gamma_{\mathrm{D}}\,, \quad \boldsymbol{\sigma}\boldsymbol{\nu} = \mathbf{0} \quad \text{on} \quad \Gamma_{\mathrm{N}}\,, \\ &\phi = \phi_{\mathrm{D}} \quad \text{on} \quad \Gamma_{\mathrm{D}}\,, \quad \text{and} \quad \widetilde{\boldsymbol{\sigma}}\cdot\boldsymbol{\nu} = 0 \quad \text{on} \quad \Gamma_{\mathrm{N}}\,, \end{aligned} \tag{2.2}$$

where $(\cdot)^{\mathtt{d}}$ denotes the deviatoric operator. The sought quantities are the Cauchy fluid pseudo-stress $\boldsymbol{\sigma}$, the average velocity of the mixture $\boldsymbol{u}$, and the volumetric fraction of the solids (in short, concentration) ϕ. In this context, the parameter β is a positive constant representing the porosity of the medium, and the permeability tensor $\boldsymbol{K} \in \mathbb{C}(\bar{\Omega}) := [C(\bar{\Omega})]^{n\times n}$ and its inverse are symmetric and uniformly positive definite, which means that there exists $\alpha_{\boldsymbol{K}} > 0$ such that

$$\boldsymbol{v}^{\mathtt{t}}\boldsymbol{K}^{-1}(\boldsymbol{x})\boldsymbol{v} \geq \alpha_{\boldsymbol{K}}|\boldsymbol{v}|^2 \quad \forall\, \boldsymbol{v} \in \mathrm{R}^n,\ \forall\, \boldsymbol{x} \in \Omega.$$

Here, we assume that the kinematic effective viscosity, μ; the one-directional Kynch batch flux density function describing hindered settling, f_{bk}; and the diffusion or sediment compressibility, ϑ; are nonlinear scalar functions of the concentration ϕ. In turn, $\boldsymbol{k}$ is a vector pointing in the direction of gravity and $\boldsymbol{f} \in \mathbf{L}^\infty(\Omega)$, $\boldsymbol{u}_{\mathrm{D}} \in \mathbf{H}^{1/2}(\Gamma_{\mathrm{D}})$, $g \in \mathrm{L}^2(\Omega)$ are given functions. For sake of the subsequent analysis, the Dirichlet datum for the concentration will be assumed homogeneous $\phi_{\mathrm{D}} = 0$; ϑ is assumed of class C^1; and we suppose that there exist positive constants μ_1, μ_2, γ_1, γ_2, ϑ_1, ϑ_2, L_μ, L_ϑ, and L_f, such that for each s, $t \in \mathrm{R}$ there holds

$$\mu_1 \leq \mu(s) \leq \mu_2\,, \quad \gamma_1 \leq f_{\mathrm{bk}}(s) \leq \gamma_2, \quad \vartheta_1 \leq \vartheta(s) \leq \vartheta_2, \tag{2.3}$$

$$|\mu(s) - \mu(t)| \leq L_\mu\,|s-t|\,, \quad |\vartheta(s) - \vartheta(t)| \leq L_\vartheta\,|s-t|\,, \quad \text{and} \quad |f_{\mathrm{bk}}(s) - f_{\mathrm{bk}}(t)| \leq L_f\,|s-t|\,. \tag{2.4}$$

2.2 The augmented mixed–primal formulation

The homogeneous Neumann and Dirichlet boundary conditions for $\boldsymbol{\sigma}$ on Γ_{N} and ϕ on Γ_{D} (second and third relations of (2.2), respectively) suggest the introduction of the following functional spaces

$$\mathbb{H}_N(\mathbf{div};\Omega) := \Big\{ \boldsymbol{\tau} \in \mathbb{H}(\mathbf{div};\Omega) : \quad \boldsymbol{\tau}\boldsymbol{\nu} = \mathbf{0} \quad \text{on} \quad \Gamma_{\mathrm{N}} \Big\},$$
$$\mathrm{H}^1_{\Gamma_{\mathrm{D}}}(\Omega) := \Big\{ \psi \in \mathrm{H}^1(\Omega) : \quad \psi = 0 \quad \text{on} \quad \Gamma_{\mathrm{D}} \Big\}.$$

Consequently, an augmented mixed-primal formulation for our original coupled problem (2.1) reads as follows: Find $(\boldsymbol{\sigma}, \boldsymbol{u}, \phi) \in \mathbb{H}_N(\mathbf{div};\Omega) \times \mathbf{H}^1(\Omega) \times \mathrm{H}^1_{\Gamma_{\mathrm{D}}}(\Omega)$ such that

$$\begin{aligned} B_\phi((\boldsymbol{\sigma},\boldsymbol{u}),(\boldsymbol{\tau},\boldsymbol{v})) &= F_\phi(\boldsymbol{\tau},\boldsymbol{v}) \quad \forall (\boldsymbol{\tau},\boldsymbol{v}) \in \mathbb{H}_N(\mathbf{div};\Omega) \times \mathbf{H}^1(\Omega)\,, \\ A_{\boldsymbol{u}}(\phi,\psi) &= G_\phi(\psi) \qquad \forall\, \psi \in \mathrm{H}^1_{\Gamma_{\mathrm{D}}}(\Omega)\,, \end{aligned} \tag{2.5}$$

where

$$\begin{aligned} B_\phi((\boldsymbol{\sigma},\boldsymbol{u}),(\boldsymbol{\tau},\boldsymbol{v})) &:= \int_\Omega \frac{1}{\mu(\phi)}\, \boldsymbol{\sigma}^{\mathtt{d}} : \boldsymbol{\tau}^{\mathtt{d}} + \int_\Omega \boldsymbol{u}\cdot\mathbf{div}\boldsymbol{\tau} - \int_\Omega \boldsymbol{v}\cdot\mathbf{div}\boldsymbol{\sigma} + \int_\Omega \boldsymbol{K}^{-1}\boldsymbol{u}\cdot\boldsymbol{v} \\ &\quad + \kappa_1 \int_\Omega \Big(\nabla \boldsymbol{u} - \frac{1}{\mu(\phi)}\, \boldsymbol{\sigma}^{\mathtt{d}} \Big) : \nabla \boldsymbol{v} - \kappa_2 \int_\Omega \boldsymbol{K}^{-1}\boldsymbol{u}\cdot\mathbf{div}\boldsymbol{\tau} + \kappa_2 \int_\Omega \mathbf{div}\boldsymbol{\sigma}\cdot\mathbf{div}\boldsymbol{\tau}\,, \end{aligned} \tag{2.6}$$

$$\begin{aligned} F_\phi(\boldsymbol{\tau},\boldsymbol{v}) &:= \langle \boldsymbol{\tau}\boldsymbol{\nu}, \boldsymbol{u}_{\mathrm{D}} \rangle_{\Gamma_{\mathrm{D}}} + \int_\Omega \boldsymbol{f}\phi\cdot\boldsymbol{v} - \kappa_2 \int_\Omega \boldsymbol{f}\phi\cdot\mathbf{div}\boldsymbol{\tau}\,, \\ A_{\boldsymbol{u}}(\phi,\psi) &:= \int_\Omega \vartheta(\phi)\,\nabla\phi\cdot\nabla\psi - \int_\Omega \phi\,\boldsymbol{u}\cdot\nabla\psi + \int_\Omega \beta\,\phi\psi \qquad \forall\, \phi,\, \psi \in \mathrm{H}^1_{\Gamma_{\mathrm{D}}}(\Omega)\,, \\ G_\phi(\psi) &:= \int_\Omega \mathfrak{f}_{\mathrm{bk}}(\phi)\,\boldsymbol{k}\cdot\nabla\psi + \int_\Omega g\psi \qquad \forall\, \psi \in \mathrm{H}^1_{\Gamma_{\mathrm{D}}}(\Omega)\,, \end{aligned} \tag{2.7}$$

and κ_1, κ_2 are positive parameters satisfying $\kappa_1 \in \Big(0, \frac{2\delta\mu_1}{\mu_2}\Big)$ and $\kappa_2 \in \Big(0, \frac{2\widetilde{\delta}\alpha_{\boldsymbol{K}}}{n\|\boldsymbol{K}^{-1}\|_\infty}\Big)$, with $\delta \in (0, 2\mu_1)$ and $\widetilde{\delta} \in \Big(0, \frac{2}{n\|\boldsymbol{K}^{-1}\|_\infty}\Big)$. Further details yielding the weak formulation (2.5), along with its fixed-point based solvability analysis can be found in [3, Section 3].

2.3 The augmented mixed–primal finite element method

We denote by $\mathcal{T}_h$ a regular partition of Ω into triangles T (resp. tetrahedra T in R^3) of diameter h_T, and meshsize $h := \max\Big\{ h_T : T \in \mathcal{T}_h \Big\}$. In addition, given an integer $k \geq 0$, $\mathrm{P}_k(T)$ denotes the space of polynomial functions on T of degree $\leq k$, and we define the corresponding local Raviart-Thomas space of order k as $\mathbf{RT}_k(T) := \mathbf{P}_k(T) \oplus \mathrm{P}_k(T)\,\boldsymbol{x}$, where, according to the notations described in Section 1, $\mathbf{P}_k(T) = [\mathrm{P}_k(T)]^n$, and $\boldsymbol{x} \in \mathrm{R}^n$. Then, the Galerkin scheme associated to (2.5), corresponds to: Find $(\boldsymbol{\sigma}_h, \boldsymbol{u}_h, \phi_h) \in \mathbb{H}^{\boldsymbol{\sigma}}_h \times \mathbf{H}^{\boldsymbol{u}}_h \times \mathrm{H}^{\phi}_h$ such that

$$\begin{aligned} B_{\phi_h}((\boldsymbol{\sigma}_h,\boldsymbol{u}_h),(\boldsymbol{\tau}_h,\boldsymbol{v}_h)) &= F_{\phi_h}(\boldsymbol{\tau}_h,\boldsymbol{v}_h) \quad \forall (\boldsymbol{\tau}_h,\boldsymbol{v}_h) \in \mathbb{H}^{\boldsymbol{\sigma}}_h \times \mathbf{H}^{\boldsymbol{u}}_h\,, \\ A_{\boldsymbol{u}_h}(\phi_h,\psi_h) &= \int_\Omega \mathfrak{f}_{\mathrm{bk}}(\phi_h)\,\boldsymbol{k}\cdot\nabla\psi_h + \int_\Omega g\psi_h \qquad \forall\, \psi_h \in \mathrm{H}^{\phi}_h\,, \end{aligned} \tag{2.8}$$

where the involved finite element spaces are defined as

$$\mathbb{H}^{\boldsymbol{\sigma}}_h := \Big\{ \boldsymbol{\tau}_h \in \mathbb{H}_N(\mathbf{div};\Omega) : \quad \mathbf{c}^{\mathtt{t}}\,\boldsymbol{\tau}_h|_T \in \mathrm{RT}_k(T) \quad \forall\, \mathbf{c} \in \mathrm{R}^n\,, \quad \forall\, T \in \mathcal{T}_h \Big\}\,,$$

$$\mathbf{H}_h^{\boldsymbol{u}} := \left\{ \boldsymbol{v}_h \in \mathbf{C}(\overline{\Omega}) : \quad \boldsymbol{v}_h|_T \in \mathbf{P}_{k+1}(T) \quad \forall\, T \in \mathcal{T}_h \right\},$$
$$\mathrm{H}_h^{\phi} := \left\{ \psi_h \in C(\overline{\Omega}) \cap \mathrm{H}^1_{\Gamma_{\mathrm{D}}}(\Omega) : \quad \psi_h|_T \in \mathrm{P}_{k+1}(T) \quad \forall\, T \in \mathcal{T}_h \right\}.$$

The solvability analysis and a priori error estimates for (2.8) have been derived in [3, Section 5].

3 A residual-based a posteriori error estimator

In this section we introduce a reliable and efficient residual-based *a posteriori* error estimator for the Galerkin scheme (2.8). In particular, as well as in [4], a Helmholtz decomposition will be employed in the corresponding proof of reliability. Even if this analysis will be restricted to the two-dimensional case using the discrete spaces from Section 2.3, an extension to the 3D case will be addressed in detail in Section 5, below.

Given a suitably chosen $r > 0$ (see [3] for details), we define the balls

$$W := \{ \phi \in \mathrm{H}^1_{\Gamma_{\mathrm{D}}}(\Omega) : \quad \|\phi\|_{1,\Omega} \leq r \} \quad \text{and} \quad W_h := \{ \phi_h \in \mathrm{H}_h^{\phi} : \quad \|\phi_h\|_{1,\Omega} \leq r \}, \tag{3.1}$$

and throughout the rest of the paper we let $(\boldsymbol{\sigma}, \boldsymbol{u}, \phi) \in \mathbb{H}_N(\mathbf{div}; \Omega) \times \mathbf{H}^1(\Omega) \times \mathrm{H}^1_{\Gamma_{\mathrm{D}}}(\Omega)$ with $\phi \in W$ and $(\boldsymbol{\sigma}_h, \boldsymbol{u}_h, \phi_h) \in \mathbb{H}_h^{\boldsymbol{\sigma}} \times \mathbf{H}_h^{\boldsymbol{u}} \times \mathrm{H}_h^{\phi}$ with $\phi_h \in W_h$ be the solutions of the continuous and discrete formulations (2.5) and (2.8), respectively. In addition, we set

$$H := \mathbb{H}_N(\mathbf{div}, \Omega) \times \mathbf{H}^1(\Omega), \qquad \|(\boldsymbol{\tau}, \boldsymbol{v})\|_H := \|\boldsymbol{\tau}\|_{\mathbf{div};\Omega} + \|\boldsymbol{v}\|_{1,\Omega} \quad \forall\, (\boldsymbol{\tau}, \boldsymbol{v}) \in H,$$

and recall from [3, Theorems 3.13 and 4.7] that the following a priori estimates hold

$$\|(\boldsymbol{\sigma}, \boldsymbol{u})\|_H \leq C_S \left\{ \|\boldsymbol{u}_{\mathrm{D}}\|_{1/2,\Gamma_{\mathrm{D}}} + \|\phi\|_{1,\Omega} \|\boldsymbol{f}\|_{\infty,\Omega} \right\},$$
$$\|(\boldsymbol{\sigma}_h, \boldsymbol{u}_h)\|_H \leq C_S \left\{ \|\boldsymbol{u}_{\mathrm{D}}\|_{1/2,\Gamma_{\mathrm{D}}} + \|\phi_h\|_{1,\Omega} \|\boldsymbol{f}\|_{\infty,\Omega} \right\},$$

where C_S is a positive constant independent of ϕ and ϕ_h.

3.1 The local error indicator

Given $T \in \mathcal{T}_h$, we let $\mathcal{E}_h(T)$ be the set of its edges, and let $\mathcal{E}_h$ be the set of all edges of the triangulation $\mathcal{T}_h$. Then we write $\mathcal{E}_h = \mathcal{E}_h(\Omega) \cup \mathcal{E}_h(\Gamma_{\mathrm{D}}) \cup \mathcal{E}_h(\Gamma_{\mathrm{N}})$, where $\mathcal{E}_h(\Omega) := \{e \in \mathcal{E}_h : e \subseteq \Omega\}$, $\mathcal{E}_h(\Gamma_{\mathrm{D}}) := \{e \in \mathcal{E}_h : e \subseteq \Gamma_{\mathrm{D}}\}$ and $\mathcal{E}_h(\Gamma_{\mathrm{N}}) := \{e \in \mathcal{E}_h : e \subseteq \Gamma_{\mathrm{N}}\}$. Also, for each edge $e \in \mathcal{E}_h$ we fix a unit normal vector $\boldsymbol{\nu}_e := (\nu_1, \nu_2)^{\mathtt{t}}$, and let $\boldsymbol{s}_e := (-\nu_2, \nu_1)^{\mathtt{t}}$ be the corresponding fixed unit tangential vector along e. Then, given $e \in \mathcal{E}_h(\Omega)$ and $\boldsymbol{v} \in \mathbf{L}^2(\Omega)$ such that $\boldsymbol{v}|_T \in \mathbf{C}(T)$ on each $T \in \mathcal{T}_h$, we let $[\![\boldsymbol{v} \cdot \boldsymbol{\nu}_e]\!]$ be the corresponding jump across e, that is, $[\![\boldsymbol{v} \cdot \boldsymbol{\nu}_e]\!] := (\boldsymbol{v}|_T - \boldsymbol{v}|_{T'})|_e \cdot \boldsymbol{\nu}_e$, where T and T' are the triangles of $\mathcal{T}_h$ having e as a common edge. Similarly, given a tensor field $\boldsymbol{\tau} \in \mathbb{L}^2(\Omega)$ such that $\boldsymbol{\tau}|_T \in \mathbb{C}(T)$ on each $T \in \mathcal{T}_h$, we let $[\![\boldsymbol{\tau} \boldsymbol{s}_e]\!]$ be the corresponding jump across e, that is, $[\![\boldsymbol{\tau} \boldsymbol{s}_e]\!] := (\boldsymbol{\tau}|_T - \boldsymbol{\tau}|_{T'})|_e \, \boldsymbol{s}_e$. If no confusion arises, we will simple write $\boldsymbol{s}$ and $\boldsymbol{\nu}$ instead $\boldsymbol{s}_e$ and $\boldsymbol{\nu}_e$, respectively.

Moreover, given scalar, vector, and tensor valued fields v, $\boldsymbol{\varphi} := (\varphi_1, \varphi_2)$ and $\boldsymbol{\tau} := (\tau_{ij})$, respectively, we denote

$$\mathbf{curl}(v) := \begin{pmatrix} \frac{\partial v}{\partial x_2} \\ -\frac{\partial v}{\partial x_1} \end{pmatrix}, \quad \underline{\mathbf{curl}}(\boldsymbol{\varphi}) := \begin{pmatrix} \mathbf{curl}(\varphi_1)^{\mathtt{t}} \\ \mathbf{curl}(\varphi_2)^{\mathtt{t}} \end{pmatrix}, \quad \text{and} \quad \mathbf{curl}(\boldsymbol{\tau}) := \begin{pmatrix} \frac{\partial \tau_{12}}{\partial x_1} - \frac{\partial \tau_{11}}{\partial x_2} \\ \frac{\partial \tau_{22}}{\partial x_1} - \frac{\partial \tau_{21}}{\partial x_2} \end{pmatrix}.$$

Then we let $\widetilde{\boldsymbol{\sigma}}_h := \vartheta(\phi_h)\nabla\phi_h - \phi_h\boldsymbol{u}_h - f_{\rm bk}(\phi_h)\boldsymbol{k}$ and define for each $T \in \mathcal{T}_h$ a local error indicator as follows

$$\begin{aligned}\theta_T^2 :=& \|\boldsymbol{f}\phi_h - (\boldsymbol{K}^{-1}\boldsymbol{u}_h - \mathbf{div}\boldsymbol{\sigma}_h)\|_{0,T}^2 + \left\|\nabla\boldsymbol{u}_h - \frac{1}{\mu(\phi_h)}\boldsymbol{\sigma}_h^{\mathtt{d}}\right\|_{0,T}^2 + h_T^2\,\|g - (\beta\phi_h - \operatorname{div}\widetilde{\boldsymbol{\sigma}}_h)\|_{0,T}^2 \\ &+ h_T^2\left\|\mathbf{curl}\left\{\frac{1}{\mu(\phi_h)}\boldsymbol{\sigma}_h^{\mathtt{d}}\right\}\right\|_{0,T}^2 + \sum_{e\in\mathcal{E}_h(T)\cap\mathcal{E}_h(\Omega)} h_e\left\|\left[\!\left[\frac{1}{\mu(\phi_h)}\boldsymbol{\sigma}_h^{\mathtt{d}}\,\boldsymbol{s}\right]\!\right]\right\|_{0,e}^2 \\ &+ \sum_{e\in\mathcal{E}_h(T)\cap\mathcal{E}_h(\Omega)} h_e\,\|[\![\widetilde{\boldsymbol{\sigma}}_h\cdot\boldsymbol{\nu}_e]\!]\|_{0,e}^2 + \sum_{e\in\mathcal{E}_h(T)\cap\mathcal{E}_h(\Gamma_{\rm N})} h_e\,\|\widetilde{\boldsymbol{\sigma}}_h\cdot\boldsymbol{\nu}\|_{0,e}^2 \\ &+ \sum_{e\in\mathcal{E}_h(T)\cap\mathcal{E}_h(\Gamma_{\rm D})}\|\boldsymbol{u}_{\rm D}-\boldsymbol{u}_h\|_{0,e}^2 + \sum_{e\in\mathcal{E}_h(T)\cap\mathcal{E}_h(\Gamma_{\rm D})} h_e\left\|\frac{d\boldsymbol{u}_{\rm D}}{d\boldsymbol{s}} - \frac{1}{\mu(\phi_h)}\boldsymbol{\sigma}_h^{\mathtt{d}}\,\boldsymbol{s}\right\|_{0,e}^2.\end{aligned} \tag{3.2}$$

We remark that the last term defining θ_T^2 requires that $\left.\dfrac{d\boldsymbol{u}_{\rm D}}{d\boldsymbol{s}}\right|_e \in \mathbf{L}^2(e)$ for each $e \in \mathcal{E}_h(\Gamma_{\rm D})$. This is fixed by assuming from now on that $\boldsymbol{u}_{\rm D} \in \mathbf{H}^1_0(\Gamma_{\rm D})$. In turn, it is not difficult to see that each term defining θ_T^2 has a residual character, and hence, proceeding as usual, a *global* residual error estimator can be defined as

$$\boldsymbol{\theta} := \left\{\sum_{T\in\mathcal{T}_h}\theta_T^2\right\}^{1/2}. \tag{3.3}$$

3.2 Reliability

Throughout the rest of the paper we assume that $\Gamma_{\rm N}$ is contained in the boundary of a convex extension of Ω, that is, there exists a convex domain B such that $\Omega \subseteq B$ and $\Gamma_{\rm N} \subseteq \partial B$ (see, e.g. [20, Theorem 3.2 and Figure 3.1]). Furthermore, according to the regularity estimate given in [3, eq. (3.24)], we also suppose from now on that $g \in \mathrm{H}^{\delta}(\Omega)$ for some $\delta \in (0,1)$. Then the main result of this section is stated as follows.

Theorem 3.1 *Assume that Ω is a connected domain and that $\boldsymbol{u}_{\rm D}$, $\Gamma_{\rm N}$, and g are as stated above. In addition, assume that the data $\boldsymbol{k}$, g, ϑ, $\boldsymbol{u}_{\rm D}$, and $\boldsymbol{f}$ are sufficiently small so that there holds*

$$C_4\,|\boldsymbol{k}| + C_5\,\|g\|_{\delta,\Omega} + C_6\,\vartheta_2 + C_7\,\|\boldsymbol{u}_{\rm D}\|_{1/2+\delta,\Gamma_{\rm D}} + C_8\,\|\boldsymbol{f}\|_{\infty,\Omega} < \frac{1}{2}, \tag{3.4}$$

where the involved constants are made precise in (3.12), below. Then, there exists a constant $C_{\mathtt{rel}} > 0$, which depends only on the model parameters, on $\|\boldsymbol{u}_{\rm D}\|_{1/2+\delta,\Gamma_{\rm D}}$, $\|\boldsymbol{f}\|_{\infty,\Omega}$, and possibly other constants, but all independent of h, such that

$$\|\phi-\phi_h\|_{1,\Omega} + \|(\boldsymbol{\sigma},\boldsymbol{u}) - (\boldsymbol{\sigma}_h,\boldsymbol{u}_h)\|_H \le C_{\mathtt{rel}}\,\boldsymbol{\theta}. \tag{3.5}$$

A couple of preliminary estimates aiming to prove (3.5) are given in the following two subsections.

3.2.1 A preliminary estimate for $\|(\boldsymbol{\sigma},\boldsymbol{u}) - (\boldsymbol{\sigma}_h,\boldsymbol{u}_h)\|_H$

In order to simplify the subsequent writing, we introduce in advance the following constants

$$C_0 := \frac{1}{\alpha(\Omega)}, \quad C_1 := 2\,C_0\,C_\delta\,\widetilde{C}_\delta\,\widehat{C}_S(r)\frac{L_\mu(1+\kappa_1^2)^{1/2}}{\mu_1^2}, \quad C_2 := C_0\,(1+\kappa_2^2)^{1/2} + r\,C_1, \tag{3.6}$$

where $\widehat{C}_S(r)$ and C_δ, $\widetilde{C}_\delta$ are defined in [3, eq. (3.23)] and [3, Lemma 3.6 and Theorem 3.10], respectively.

Lemma 3.2 *Let* $\boldsymbol{\theta}_0^2 := \sum_{T\in\mathcal{T}_h} \theta_{0,T}^2$, *where for each* $T \in \mathcal{T}_h$ *we set*

$$\theta_{0,T}^2 := \|\boldsymbol{f}\phi_h - (\boldsymbol{K}^{-1}\boldsymbol{u}_h - \mathbf{div}\boldsymbol{\sigma}_h)\|_{0,T}^2 + \left\|\nabla\boldsymbol{u}_h - \frac{1}{\mu(\phi_h)}\boldsymbol{\sigma}_h^{\mathtt{d}}\right\|_{0,T}^2 . \tag{3.7}$$

Then there exists $\bar{C} > 0$, *depending on* C_0, κ_1, *such that*

$$\|(\boldsymbol{\sigma},\boldsymbol{u})-(\boldsymbol{\sigma}_h,\boldsymbol{u}_h)\|_H \leq \bar{C}\left\{\boldsymbol{\theta}_0+\|E_h\|_{\mathbb{H}_N(\mathbf{div},\Omega)'}\right\}+\left\{C_1\,\|\boldsymbol{u}_{\mathrm{D}}\|_{1/2+\delta,\Gamma_{\mathrm{D}}}+C_2\,\|\boldsymbol{f}\|_{\infty,\Omega}\right\}\|\phi-\phi_h\|_{1,\Omega}\,, \tag{3.8}$$

where C_1 *and* C_2 *are given by* (3.6), *and the functional* $E_h \in \mathbb{H}_N(\mathbf{div},\Omega)'$ *is defined by*

$$\begin{aligned} E_h(\boldsymbol{\zeta}) := \langle\boldsymbol{\zeta}\,\boldsymbol{\nu},\boldsymbol{u}_{\mathrm{D}}\rangle_{\Gamma_{\mathrm{D}}} - \int_\Omega \frac{1}{\mu(\phi_h)}\boldsymbol{\sigma}_h^{\mathtt{d}} : \boldsymbol{\zeta} - \int_\Omega \boldsymbol{u}_h\cdot\mathbf{div}\boldsymbol{\zeta} \\ -\kappa_2\int_\Omega(\boldsymbol{f}\phi_h - (\boldsymbol{K}^{-1}\boldsymbol{u}_h - \mathbf{div}\boldsymbol{\sigma}_h))\cdot\mathbf{div}\boldsymbol{\zeta} \qquad \forall\,\boldsymbol{\zeta}\in\mathbb{H}_N(\mathbf{div},\Omega)\,. \end{aligned} \tag{3.9}$$

In addition, there holds

$$E_h(\boldsymbol{\zeta}_h) = 0 \qquad \forall\,\boldsymbol{\zeta}_h \in \mathbb{H}_h^{\boldsymbol{\sigma}}\,. \tag{3.10}$$

Proof. Even though the present bilinear form B_ϕ (*cf.* (2.6)) and the corresponding one from [4, eq. (2.9)] differ in a couple of linear terms, the present proof is almost verbatim as [4, Lemma 3.2], particularly concerning the application of the H-ellipticity (see [3, Lemma 3.3]) of B_ϕ to the error $(\boldsymbol{\sigma},\boldsymbol{u})-(\boldsymbol{\sigma}_h,\boldsymbol{u}_h)$, and the estimates for $|B_{\phi_h}(\,\cdot\,,(\boldsymbol{\zeta},\boldsymbol{w}))-B_\phi(\,\cdot\,,(\boldsymbol{\zeta},\boldsymbol{w}))|$ and $|F_\phi(\boldsymbol{\zeta},\boldsymbol{w})-F_{\phi_h}(\boldsymbol{\zeta},\boldsymbol{w})|$, and hence further details are omitted. □

Observe, according to (3.10), that for each $\boldsymbol{\zeta}\in\mathbb{H}_N(\mathbf{div},\Omega)$ we can write

$$E_h(\boldsymbol{\zeta}) \;=\; E_h(\boldsymbol{\zeta}-\boldsymbol{\zeta}_h) \qquad \forall\,\boldsymbol{\zeta}_h\in\mathbb{H}_h^{\boldsymbol{\sigma}}\,,$$

and hence the upper bound of $\|E_h\|_{\mathbb{H}_N(\mathbf{div},\Omega)'}$ to be derived below (see Section 3.2.3) will employ the foregoing expression with a suitable choice of $\boldsymbol{\zeta}_h\in\mathbb{H}_h^{\boldsymbol{\sigma}}$.

We end this section with an alternative expression for the functional E_h, which will be used later on in Section 3.2.4 to obtain a partial estimate for Θ, and then in Section 4 to derive a second a posteriori error estimator. In fact, integrating by parts the expression $\displaystyle\int_\Omega \boldsymbol{u}_h\cdot\mathbf{div}\boldsymbol{\zeta}$, and using the homogeneous Neumann boundary condition on Γ_{N}, we find that E_h can be rewritten as

$$\begin{aligned} E_h(\boldsymbol{\zeta}) := \langle\boldsymbol{\zeta}\,\boldsymbol{\nu},\boldsymbol{u}_{\mathrm{D}}-\boldsymbol{u}_h\rangle_{\Gamma_{\mathrm{D}}} + \int_\Omega\left(\nabla\boldsymbol{u}_h - \frac{1}{\mu(\phi_h)}\boldsymbol{\sigma}_h^{\mathtt{d}}\right):\boldsymbol{\zeta} \\ -\kappa_2\int_\Omega(\boldsymbol{f}\phi_h - (\boldsymbol{K}^{-1}\boldsymbol{u}_h - \mathbf{div}\boldsymbol{\sigma}_h))\cdot\mathbf{div}\boldsymbol{\zeta} \qquad \forall\,\boldsymbol{\zeta}\in\mathbb{H}_N(\mathbf{div},\Omega)\,. \end{aligned} \tag{3.11}$$

3.2.2 A preliminary estimate for $\|\phi-\phi_h\|_{1,\Omega}$

In contrast with [4, Section 3.2.2], in this section we establish an estimate for the error $\|\phi-\phi_h\|_{1,\Omega}$ by employing the ellipticity of the bilinear form $A_{\phi,\boldsymbol{u}}$ [3, eq. (3.13)]. The reason of the latter is due to fact that the Gâteaux derivative of the nonlinear induced operator by the form $A_{\boldsymbol{u}}$ (*cf.* (2.7)) is

not elliptic as it was in [4], and hence we can not apply [4, Lemma 3.4] to derive the corresponding preliminary bound. In light of the above, we now set the following constants

$$\begin{aligned} &\widetilde{C} := \frac{1}{\widetilde{\alpha}}, \quad C_3 := L_\vartheta\, C_\delta\, \widetilde{C}_\delta\, \widehat{C}_{\widetilde{S}}(r), \quad C_4 := \widetilde{C}\,(L_f + C_3\,\gamma_2|\Omega|^{1/2}), \quad C_5 := \widetilde{C}\,C_3, \\ &C_6 := 2\,\widetilde{C}, \quad C_7 := r\,c(\Omega)\,\widetilde{C}\,C_1, \quad C_8 := r\,c(\Omega)\,\widetilde{C}\,C_2, \quad C_9 := r\,c(\Omega)\,\bar{C}, \end{aligned} \tag{3.12}$$

where $\widehat{C}_{\widetilde{S}}(r)$, C_δ, $\widetilde{C}_\delta$ and $\bar{C}$ are the constants provided by [3, eq. (3.24)], [3, Lemma 3.7, Theorem 3.10], and Lemma 3.2, respectively.

Lemma 3.3 *Assume that the data $\boldsymbol{k}$, g, ϑ, $\boldsymbol{u}_{\mathrm{D}}$, and $\boldsymbol{f}$ are sufficiently small so that there holds*

$$C_4\,|\boldsymbol{k}| + C_5\,\|g\|_{\delta,\Omega} + C_6\,\vartheta_2 + C_7\,\|\boldsymbol{u}_{\mathrm{D}}\|_{1/2+\delta,\Gamma_{\mathrm{D}}} + C_8\,\|\boldsymbol{f}\|_{\infty,\Omega} < \frac{1}{2}. \tag{3.13}$$

Then, there exists $\widehat{C} > 0$, depending on $\widetilde{C}$ and C_9 (cf. (3.12)), such that

$$\|\phi - \phi_h\|_{1,\Omega} \leq \widehat{C}\left\{\boldsymbol{\theta}_0 + \|E_h\|_{\mathbb{H}_N(\mathbf{div},\Omega)'} + \|\widetilde{E}_h\|_{\mathrm{H}^1_{\Gamma_{\mathrm{D}}}(\Omega)'}\right\}, \tag{3.14}$$

where $\boldsymbol{\theta}_0$ and E_h are given in the statement of Lemma 3.2 and (3.9), respectively, and $\widetilde{E}_h \in \mathrm{H}^1_{\Gamma_{\mathrm{D}}}(\Omega)'$ is defined for each $\psi \in \mathrm{H}^1_{\Gamma_{\mathrm{D}}}(\Omega)$ by

$$\widetilde{E}_h(\psi) := \int_\Omega (g - \beta\,\phi_h)\,\psi - \int_\Omega \left\{\vartheta(\phi_h)\,\nabla\phi_h - \phi_h\,\boldsymbol{u}_h - f_{\mathrm{bk}}(\phi_h)\,\boldsymbol{k}\right\}\cdot\nabla\psi\,. \tag{3.15}$$

In addition, there holds

$$\widetilde{E}_h(\psi_h) = 0 \qquad \forall\,\psi_h \in \mathrm{H}^\phi_h\,. \tag{3.16}$$

Proof. We begin by recalling, from [3, Lemma 3.4], that the bilinear form

$$A_{\phi,\boldsymbol{u}}(\varphi,\psi) := \int_\Omega \vartheta(\phi)\,\nabla\varphi\cdot\nabla\psi - \int_\Omega \varphi\,\boldsymbol{u}\cdot\nabla\psi + \int_\Omega \beta\,\varphi\,\psi \quad \forall\,\varphi,\psi \in \mathrm{H}^1_{\Gamma_{\mathrm{D}}}(\Omega), \tag{3.17}$$

is $\mathrm{H}^1_{\Gamma_{\mathrm{D}}}(\Omega)$-elliptic with constant $\widetilde{\alpha} := \frac{\vartheta_1}{2\,c_p^2}$, from which we deduce the following global inf-sup condition

$$\widetilde{\alpha}\,\|\varphi\|_{1,\Omega} \leq \sup_{\substack{\psi\in\mathrm{H}^1_{\Gamma_{\mathrm{D}}}(\Omega)\\ \psi\neq 0}} \frac{A_{\phi,\boldsymbol{u}}(\varphi,\psi)}{\|\psi\|_{1,\Omega}} \qquad \forall\,\varphi \in \mathrm{H}^1_{\Gamma_{\mathrm{D}}}(\Omega). \tag{3.18}$$

Next, applying (3.18) to the Galerkin error $\varphi := \phi - \phi_h$, we find that

$$\widetilde{\alpha}\,\|\phi - \phi_h\|_{1,\Omega} \leq \sup_{\substack{\psi\in\mathrm{H}^1_{\Gamma_{\mathrm{D}}}(\Omega)\\ \psi\neq 0}} \frac{A_{\phi,\boldsymbol{u}}(\phi,\psi) - A_{\phi,\boldsymbol{u}}(\phi_h,\psi)}{\|\psi\|_{1,\Omega}}. \tag{3.19}$$

Now, using the fact that $A_{\phi,\boldsymbol{u}}(\phi,\psi) = A_{\boldsymbol{u}}(\phi,\psi) = G_\phi(\psi)$, and adding and subtracting suitable terms, it follows that

$$A_{\phi,\boldsymbol{u}}(\phi,\psi) - A_{\phi,\boldsymbol{u}}(\phi_h,\psi) = G_\phi(\psi) - G_{\phi_h}(\psi) + G_{\phi_h}(\psi) - A_{\boldsymbol{u}_h}(\phi_h,\psi) + A_{\boldsymbol{u}_h}(\phi_h,\psi) - A_{\phi,\boldsymbol{u}}(\phi_h,\psi)\,. \tag{3.20}$$

In turn, using the definition of $A_{\boldsymbol{u}_h}$ (*cf.* (2.7)) and $A_{\phi,\boldsymbol{u}}$ (*cf.* (3.17)), we find that

$$\begin{aligned} A_{\boldsymbol{u}_h}(\phi_h,\psi) - A_{\phi,\boldsymbol{u}}(\phi_h,\psi) &= \int_\Omega (\vartheta(\phi) - \vartheta(\phi_h))\,\nabla(\phi - \phi_h)\cdot\nabla\psi \\ &+ \int_\Omega \phi_h\,(\boldsymbol{u} - \boldsymbol{u}_h)\cdot\nabla\psi - \int_\Omega (\vartheta(\phi) - \vartheta(\phi_h))\,\nabla\phi\cdot\nabla\psi, \end{aligned} \tag{3.21}$$

from which, employing the upper bound of ϑ (*cf.* (2.3)), (3.1), and proceeding as in [3, eq. (5.13)-(5.14)] on the third term to the right hand side of (3.21), we arrive at

$$|A_{\boldsymbol{u}_h}(\phi_h,\psi) - A_{\phi,\boldsymbol{u}}(\phi_h,\psi)| \leq \left\{ 2\,\vartheta_2 + C_3\left(\gamma_2\,|\Omega|^{1/2}\,|\boldsymbol{k}| + \|g\|_{\delta,\Omega}\right)\right\}\|\phi-\phi_h\|_{1,\Omega}\,|\psi|_{1,\Omega} + r\,c(\Omega)\,\|\boldsymbol{u}-\boldsymbol{u}_h\|_{1,\Omega}\,|\psi|_{1,\Omega}\,. \tag{3.22}$$

Thus, applying the estimate for $|G_\phi(\psi) - G_{\phi_h}(\psi)|$ (see [3, eq. (5.12)]) and estimate (3.22), we obtain from (3.19) and (3.20) that

$$\|\phi-\phi_h\|_{1,\Omega} \leq \widetilde{C}\,\|G_{\phi_h} - A_{\boldsymbol{u}_h}(\phi_h,\cdot)\|_{\mathrm{H}^1_{\Gamma_{\mathrm{D}}}(\Omega)'} + \left\{C_4|\boldsymbol{k}| + C_5\|g\|_{\delta,\Omega} + C_6\vartheta_2\right\}\|\phi-\phi_h\|_{1,\Omega} + r\,c(\Omega)\,\widetilde{C}\,\|\boldsymbol{u}-\boldsymbol{u}_h\|_{1,\Omega}\,.$$

Then, bounding $\|\boldsymbol{u}-\boldsymbol{u}_h\|_{1,\Omega}$ by the error estimate provided by (3.8) (*cf.* Lemma 3.2), and employing (3.13), we deduce that

$$\|\phi-\phi_h\|_{1,\Omega} \leq 2\,\widetilde{C}\left\{\|G_{\phi_h} - A_{\boldsymbol{u}_h}(\phi_h,\cdot)\|_{\mathrm{H}^1_{\Gamma_{\mathrm{D}}}(\Omega)'} + C_9\left(\boldsymbol{\theta}_0 + \|E_h\|_{\mathbb{H}_N(\mathbf{div},\Omega)'}\right)\right\}, \tag{3.23}$$

where, bearing in mind (3.15), there holds

$$G_{\phi_h} - A_{\boldsymbol{u}_h}(\phi_h,\cdot) = \widetilde{E}_h\,,$$

and hence (3.23) yields (3.14). Finally, using the fact that $G_{\phi_h}(\psi_h) - A_{\boldsymbol{u}_h}(\phi_h,\psi_h) = 0 \quad \forall \psi_h \in \mathrm{H}^\phi_h$, we obtain (3.16) and the proof concludes. □

We observe here that the upper bound in the assumption (3.13) could have been taken as any constant in $(0,1)$. We have chosen $\frac{1}{2}$ for simplicity and also in order to minimize the resulting constant $\widehat{C}$ in (3.14). Furthermore, it is important to remark, according to (3.16), that for each $\psi \in \mathrm{H}^1_{\Gamma_{\mathrm{D}}}(\Omega)$ there holds $\widetilde{E}_h(\psi) = \widetilde{E}_h(\psi - \psi_h) \quad \forall\, \psi_h \in \mathrm{H}^\phi_h$, and therefore $\|\widetilde{E}_h\|_{\mathrm{H}^1_{\Gamma_{\mathrm{D}}}(\Omega)'}$ will be estimated below (see Subsection 3.2.3) by employing the foregoing expression with a suitable choice of $\psi_h \in \mathrm{H}^\phi_h$.

3.2.3 A preliminary estimate for the total error

We now combine the inequalities provided by Lemmas 3.2 and 3.3 to derive a first estimate for the total error $\|\phi-\phi_h\|_{1,\Omega} + \|(\boldsymbol{\sigma},\boldsymbol{u}) - (\boldsymbol{\sigma}_h,\boldsymbol{u}_h)\|_H$. To this end, we now introduce the constants

$$C(\boldsymbol{u}_{\mathrm{D}},\boldsymbol{f}) := \widehat{C}\left\{C_1\,\|\boldsymbol{u}_{\mathrm{D}}\|_{1/2+\varepsilon,\Gamma_{\mathrm{D}}} + C_2\,\|\boldsymbol{f}\|_{\infty,\Omega} + 1\right\} \quad \text{and} \quad c(\boldsymbol{u}_{\mathrm{D}},\boldsymbol{f}) := \bar{C} + C(\boldsymbol{u}_{\mathrm{D}},\boldsymbol{f})\,,$$

where $\bar{C}$ and $\widehat{C}$ are provided by Lemmas 3.2 and 3.3, respectively, and C_1 and C_2 are given by (3.6).

Theorem 3.4 *Assume that*

$$C_4\,|\boldsymbol{k}| + C_5\,\|g\|_{\delta,\Omega} + C_6\,\vartheta_2 + C_7\,\|\boldsymbol{u}_{\mathrm{D}}\|_{1/2+\delta,\Gamma_{\mathrm{D}}} + C_8\,\|\boldsymbol{f}\|_{\infty,\Omega} < \frac{1}{2}.$$

Then there holds

$$\|\phi-\phi_h\|_{1,\Omega} + \|(\boldsymbol{\sigma},\boldsymbol{u})-(\boldsymbol{\sigma}_h,\boldsymbol{u}_h)\|_H \leq C(\boldsymbol{u}_{\mathrm{D}},\boldsymbol{f})\,\|\widetilde{E}_h\|_{\mathrm{H}^1_{\Gamma_{\mathrm{D}}}(\Omega)'} + c(\boldsymbol{u}_{\mathrm{D}},\boldsymbol{f})\left\{\boldsymbol{\theta}_0 + \|E_h\|_{\mathbb{H}_N(\mathbf{div},\Omega)'}\right\}. \tag{3.24}$$

Proof. The estimate (3.24) is obtained by replacing the upper bound for $\|\phi-\phi_h\|_{1,\Omega}$, given by (3.14), into the second term on the right hand side of (3.8), and then adding the result to the right hand side of (3.14). □

Having established the upper bound (3.24), and in order to obtain an explicit estimate for the total error, we turn to the derivation of suitable upper bounds for $\|\widetilde{E}_h\|_{\mathrm{H}^1_{\Gamma_{\mathrm{D}}}(\Omega)'}$ and $\|E_h\|_{\mathbb{H}_N(\mathbf{div},\Omega)'}$.

3.2.4 Upper bounds for $\|\widetilde{E}_h\|_{\mathrm{H}^1_{\Gamma_{\mathrm{D}}}(\Omega)'}$ and $\|E_h\|_{\mathbb{H}_N(\mathbf{div},\Omega)'}$

We begin by recalling the Clément interpolation operator $\mathcal{I}_h : \mathrm{H}^1(\Omega) \to X_h$ (*cf.* [14]), where

$$X_h := \{v_h \in C(\overline{\Omega}) : v_h|_T \in \mathrm{P}_1(T) \quad \forall T \in \mathcal{T}_h\}.$$

The following result states the local approximation properties of $\mathcal{I}_h$ (for a proof, see [14]).

Lemma 3.5 *There exist constants $c_1, c_2 > 0$, independent of h, such that for all $v \in \mathrm{H}^1(\Omega)$ there hold*

$$\|v - \mathcal{I}_h(v)\|_{0,T} \leq c_1 h_T \|v\|_{1,\Delta(T)} \quad \forall T \in \mathcal{T}_h,$$

and

$$\|v - \mathcal{I}_h(v)\|_{0,e} \leq c_2 h_e^{1/2} \|v\|_{1,\Delta(e)} \quad \forall e \in \mathcal{E}_h,$$

where $\Delta(T)$ and $\Delta(e)$ are the union of all elements intersecting with T and e, respectively.

We now recall the definition of the concentration flux

$$\widetilde{\boldsymbol{\sigma}}_h := \vartheta(\phi_h)\nabla\phi_h - \phi_h \boldsymbol{u}_h - f_{\mathrm{bk}}(\phi_h)\boldsymbol{k}\,. \tag{3.25}$$

Then, the following lemma provides an upper bound for $\|\widetilde{E}_h\|_{\mathrm{H}^1_{\Gamma_{\mathrm{D}}}(\Omega)'}$.

Lemma 3.6 *Let $\widetilde{\boldsymbol{\eta}}^2 := \sum_{T\in\mathcal{T}_h} \widetilde{\eta}_T^2$, where for each $T \in \mathcal{T}_h$ we set*

$$\widetilde{\eta}_T^2 := h_T^2 \|g - (\beta\phi_h - \operatorname{div}\widetilde{\boldsymbol{\sigma}}_h)\|_{0,T}^2 + \sum_{e\in\mathcal{E}_h(T)\cap\mathcal{E}_h(\Omega)} h_e \|[\![\widetilde{\boldsymbol{\sigma}}_h \cdot \boldsymbol{\nu}_e]\!]\|_{0,e}^2 + \sum_{e\in\mathcal{E}_h(T)\cap\mathcal{E}_h(\Gamma_{\mathrm{N}})} h_e \|\widetilde{\boldsymbol{\sigma}}_h \cdot \boldsymbol{\nu}\|_{0,e}^2\,.$$

Then there exists $c > 0$, independent of h, such that

$$\|\widetilde{E}_h\|_{\mathrm{H}^1_{\Gamma_{\mathrm{D}}}(\Omega)'} \leq c\,\widetilde{\boldsymbol{\eta}}\,. \tag{3.26}$$

Proof. It corresponds to a slight modification in the proof of [4, Lemma 3.8]. □

Our next goal is to provide an upper bound for $\|E_h\|_{\mathbb{H}_N(\mathbf{div},\Omega)'}$ (*cf.* (3.9)), which, being less straightforward than Lemma 3.6, requires several preliminary results. To this end, we start by introducing the space

$$\mathbf{H}^1_{\Gamma_{\mathrm{N}}}(\Omega) := \left\{\boldsymbol{\varphi} \in \mathbf{H}^1(\Omega) : \quad \boldsymbol{\varphi} = \mathbf{0} \quad \text{on} \quad \Gamma_{\mathrm{N}}\right\},$$

and establishing a suitable Helmholtz decomposition of our space $\mathbb{H}_N(\mathbf{div},\Omega)$.

Lemma 3.7 *Assume that Ω is a connected domain and that Γ_{N} is contained in the boundary of a convex extension of Ω. Then, for each $\boldsymbol{\zeta} \in \mathbb{H}_N(\mathbf{div},\Omega)$, there exist $\boldsymbol{\tau} \in \mathbb{H}^1(\Omega)$ and $\boldsymbol{\chi} \in \mathbf{H}^1_{\Gamma_{\mathrm{N}}}(\Omega)$ such that*

$$\boldsymbol{\zeta} = \boldsymbol{\tau} + \underline{\mathbf{curl}}(\boldsymbol{\chi}) \quad \text{in} \quad \Omega\,, \tag{3.27}$$

and

$$\|\boldsymbol{\tau}\|_{1,\Omega} + \|\boldsymbol{\chi}\|_{1,\Omega} \leq C\,\|\boldsymbol{\zeta}\|_{\mathbf{div},\Omega}\,, \tag{3.28}$$

with a positive constant C independent of $\boldsymbol{\zeta}$.

Proof. See [4, Lemma 3.9]. □

We continue our analysis by introducing the following finite element subspace of $\mathbf{H}_{\Gamma_N}(\Omega)$

$$\mathbf{X}_{h,N} := \Big\{ \boldsymbol{\varphi}_h \in \mathbf{C}(\overline{\Omega}) : \quad \boldsymbol{\varphi}_h|_T \in \mathbf{P}_1(T) \quad \forall\, T \in \mathcal{T}_h, \quad \boldsymbol{\varphi}_h = \mathbf{0} \text{ on } \Gamma_N \Big\},$$

and considering, analogously as before, the Clément interpolation operator $\boldsymbol{\mathcal{I}}_{h,N} : \mathbf{H}_{\Gamma_N}(\Omega) \to \mathbf{X}_{h,N}$. In addition, we let $\Pi_h : \mathbb{H}^1(\Omega) \to \mathbb{H}_h^{\boldsymbol{\sigma}}$ be the Raviart-Thomas interpolation operator (see [9],[29]), which, according to its characterization properties (see e.g. [19, Section 3.4.1]), verifies

$$\mathbf{div}(\Pi_h(\bar{\boldsymbol{\tau}})) = \mathcal{P}_h(\mathbf{div}\bar{\boldsymbol{\tau}}) \qquad \forall\, \bar{\boldsymbol{\tau}} \in \mathbb{H}^1(\Omega), \tag{3.29}$$

where $\mathcal{P}_h : \mathbf{L}^2(\Omega) \to \mathbf{Q}_h$ is the $\mathbf{L}^2(\Omega)$-orthogonal projector and

$$\mathbf{Q}_h := \big\{ \boldsymbol{v} \in \mathbf{L}^2(\Omega) : \quad \boldsymbol{v}|_T \in \mathbf{P}_k(T) \quad \forall\, T \in \mathcal{T}_h \big\}.$$

Further approximation properties of Π_h are summarized as follows (see [19, Lemmas 3.16 and 3.18]).

Lemma 3.8 *There exist $c_3, c_4 > 0$, independent of h, such that for all $\bar{\boldsymbol{\tau}} \in \mathbb{H}^1(\Omega)$ there holds*

$$\|\bar{\boldsymbol{\tau}} - \Pi_h(\bar{\boldsymbol{\tau}})\|_{0,T} \leq c_3\, h_T\, \|\bar{\boldsymbol{\tau}}\|_{1,T} \quad \forall\, T \in \mathcal{T}_h\,,$$

and

$$\|(\bar{\boldsymbol{\tau}} - \Pi_h(\bar{\boldsymbol{\tau}}))\,\boldsymbol{\nu}\|_{0,e} \leq c_4\, h_e^{1/2}\, \|\bar{\boldsymbol{\tau}}\|_{1,T_e} \quad \forall\, e \in \mathcal{E}_h(\Omega) \cup \mathcal{E}_h(\Gamma_D)\,,$$

where T_e is a triangle of $\mathcal{T}_h$ containing the edge e on its boundary.

Next, given $\boldsymbol{\zeta} \in \mathbb{H}_N(\mathbf{div}, \Omega)$ and its Helmholtz decomposition (3.27), we define $\boldsymbol{\chi}_h := \boldsymbol{\mathcal{I}}_{h,N}(\boldsymbol{\chi})$, and set

$$\boldsymbol{\zeta}_h := \Pi_h(\boldsymbol{\tau}) + \underline{\mathbf{curl}}(\boldsymbol{\chi}_h) \in \mathbb{H}_h^{\boldsymbol{\sigma}} \tag{3.30}$$

as its associated discrete Helmholtz decomposition. Then, from (3.27) and (3.30), it follows that

$$\boldsymbol{\zeta} - \boldsymbol{\zeta}_h = \boldsymbol{\tau} - \Pi_h(\boldsymbol{\tau}) + \underline{\mathbf{curl}}(\boldsymbol{\chi} - \boldsymbol{\chi}_h)\,.$$

Therefore, according to (3.9) and (3.10), we deduce that

$$E_h(\boldsymbol{\zeta}) = E_h(\boldsymbol{\zeta} - \boldsymbol{\zeta}_h) = E_h(\boldsymbol{\tau} - \Pi_h(\boldsymbol{\tau})) + E_h(\underline{\mathbf{curl}}(\boldsymbol{\chi} - \boldsymbol{\chi}_h))\,. \tag{3.31}$$

Notice from (3.31) that, in order to estimate $\|E_h\|_{\mathbb{H}_N(\mathbf{div},\Omega)'}$, it only remains to bound $|E_h(\boldsymbol{\tau} - \Pi_h(\boldsymbol{\tau}))|$ and $|E_h(\underline{\mathbf{curl}}(\boldsymbol{\chi} - \boldsymbol{\chi}_h))|$ in terms of a multiple of $\|\boldsymbol{\zeta}\|_{\mathbf{div},\Omega}$, which is done in the rest of the present Section 3.2.4. To this end, we now recall from [16] the following integration by parts formula on the boundary.

Lemma 3.9 *There holds*

$$\langle \underline{\mathbf{curl}}\,\boldsymbol{\chi}\,\boldsymbol{\nu}, \boldsymbol{\phi} \rangle = -\langle \frac{d\boldsymbol{\phi}}{d\boldsymbol{s}}, \boldsymbol{\chi} \rangle \qquad \forall\, \boldsymbol{\chi}, \boldsymbol{\phi} \in \mathbf{H}^1(\Omega). \tag{3.32}$$

Proof. It follows from suitable applications of the Green formulae provided in [25, Chapter I, eq. (2.17) and Theorem 2.11]. □

Lemma 3.10 *Let* $\boldsymbol{\theta}_1^2 := \sum_{T\in\mathcal{T}_h} \theta_{1,T}^2$, *where for each* $T \in \mathcal{T}_h$ *we set*

$$\theta_{1,T}^2 := h_T^2 \left\| \mathbf{curl}\left\{ \frac{1}{\mu(\phi_h)} \boldsymbol{\sigma}_h^{\mathtt{d}} \right\} \right\|_{0,T}^2 + \sum_{e\in\mathcal{E}_h(T)\cap\mathcal{E}_h(\Omega)} h_e \left\| \left[\!\!\left[\frac{1}{\mu(\phi_h)} \boldsymbol{\sigma}_h^{\mathtt{d}} \boldsymbol{s} \right]\!\!\right] \right\|_{0,e}^2$$
$$+ \sum_{e\in\mathcal{E}_h(T)\cap\mathcal{E}_h(\Gamma_{\mathrm{D}})} h_e \left\| \frac{d\boldsymbol{u}_{\mathrm{D}}}{d\boldsymbol{s}} - \frac{1}{\mu(\phi_h)} \boldsymbol{\sigma}_h^{\mathtt{d}}\, \boldsymbol{s} \right\|_{0,e}^2 .$$

Then there exists $c > 0$, *independent of* h, *such that*

$$|E_h(\underline{\mathbf{curl}}(\boldsymbol{\chi} - \boldsymbol{\chi}_h)| \leq c\, \boldsymbol{\theta}_1\, \|\boldsymbol{\zeta}\|_{\mathbf{div},\Omega} . \tag{3.33}$$

Proof. See [4, Lemma 3.11]. □

Lemma 3.11 *Let* $\boldsymbol{\theta}_2^2 := \sum_{T\in\mathcal{T}_h} \theta_{2,T}^2$, *where for each* $T \in \mathcal{T}_h$ *we set*

$$\theta_{2,T}^2 := h_T^2 \left\| \nabla \boldsymbol{u}_h - \frac{1}{\mu(\phi_h)} \boldsymbol{\sigma}_h^{\mathtt{d}} \right\|_{0,T}^2 + \|\boldsymbol{f}\phi_h - (\boldsymbol{K}^{-1}\boldsymbol{u}_h - \mathbf{div}\boldsymbol{\sigma}_h)\|_{0,T}^2 + \sum_{e\in\mathcal{E}_h(T)\cap\mathcal{E}_h(\Gamma_{\mathrm{D}})} h_e \|\boldsymbol{u}_{\mathrm{D}} - \boldsymbol{u}_h\|_{0,e}^2 .$$

Then there exists $c > 0$, *independent of* h, *such that*

$$|E_h(\boldsymbol{\tau} - \Pi_h(\boldsymbol{\tau}))| \leq c\, \boldsymbol{\theta}_2\, \|\boldsymbol{\zeta}\|_{\mathbf{div},\Omega} . \tag{3.34}$$

Proof. Using the alternative definition of the functional E_h (*cf.* (3.11)), applying the identity (3.29), and denoting by $\mathcal{I}$ a generic identity operator, we find that

$$\begin{aligned} E_h(\boldsymbol{\tau} - \Pi_h(\boldsymbol{\tau})) \;=\; & \langle (\boldsymbol{\tau} - \Pi_h(\boldsymbol{\tau}))\, \boldsymbol{\nu}, \boldsymbol{u}_{\mathrm{D}} - \boldsymbol{u}_h \rangle_{\Gamma_{\mathrm{D}}} + \int_\Omega \left(\nabla \boldsymbol{u}_h - \frac{1}{\mu(\phi_h)} \boldsymbol{\sigma}_h^{\mathtt{d}} \right) : (\boldsymbol{\tau} - \Pi_h(\boldsymbol{\tau})) \\ & - \kappa_2 \int_\Omega (\boldsymbol{f}\phi_h - (\boldsymbol{K}^{-1}\boldsymbol{u}_h - \mathbf{div}\boldsymbol{\sigma}_h)) \cdot (\mathcal{I} - \mathcal{P}_h)(\mathbf{div}\boldsymbol{\tau}). \end{aligned} \tag{3.35}$$

Next, the first two terms on the right hand side of (3.35) are simply bounded by applying the Cauchy-Schwarz in $\mathbf{L}^2(\Gamma_{\mathrm{D}})$ and $\mathbb{L}^2(\Omega)$, and then employing the approximation properties of Π_h provided by Lemma 3.8. In turn, for the corresponding third term, it suffices to see, thanks to the Cauchy-Schwarz inequality and the stability estimate (3.28), that

$$\begin{aligned} & \left| \int_\Omega (\boldsymbol{f}\phi_h - (\boldsymbol{K}^{-1}\boldsymbol{u}_h - \mathbf{div}\boldsymbol{\sigma}_h)) \cdot (\mathcal{I} - \mathcal{P}_h)(\mathbf{div}\,\boldsymbol{\tau})) \right| \\ & \quad \leq \|\boldsymbol{f}\phi_h - (\boldsymbol{K}^{-1}\boldsymbol{u}_h - \mathbf{div}\boldsymbol{\sigma}_h)\|_{0,\Omega}\, \|\mathbf{div}\,\boldsymbol{\tau}\|_{0,\Omega} \leq \|\boldsymbol{f}\phi_h - (\boldsymbol{K}^{-1}\boldsymbol{u}_h - \mathbf{div}\boldsymbol{\sigma}_h)\|_{0,\Omega}\, \|\boldsymbol{\zeta}\|_{\mathbf{div},\Omega} , \end{aligned}$$

which ends the proof. □

By virtue of Lemmas 3.10 and 3.11 we deduce the following upper bound for $\|E_h\|_{\mathbb{H}_N(\mathbf{div},\Omega)'}$.

Lemma 3.12 *There exists* $c > 0$, *independent of* h, *such that*

$$\|E_h\|_{\mathbb{H}_N(\mathbf{div},\Omega)'} \leq c \left\{ \boldsymbol{\theta}_1 + \boldsymbol{\theta}_2 \right\} .$$

Proof. It follows straightforwardly from (3.31) and the upper bounds (3.33) and (3.34). □

At this point we remark that the terms $h_T^2\|\nabla \boldsymbol{u}_h - \frac{1}{\mu(\phi_h)}\boldsymbol{\sigma}_h^{\mathtt{d}}\|_{0,T}^2$ and $h_e\|\boldsymbol{u}_{\mathrm{D}} - \boldsymbol{u}_h\|_{0,e}^2$, which appear in the definition of $\theta_{2,T}^2$ (*cf.* Lemma 3.11), are dominated by $\|\nabla \boldsymbol{u}_h - \frac{1}{\mu(\phi_h)}\boldsymbol{\sigma}_h^{\mathtt{d}}\|_{0,T}^2$ and $\|\boldsymbol{u}_{\mathrm{D}} - \boldsymbol{u}_h\|_{0,e}^2$, respectively, which form part of $\theta_{0,T}^2$ (*cf.* (3.7)). Therefore, the reliability estimate (3.5) (*cf.* Theorem 3.1) is a direct consequence of Theorem 3.4, the definition of $\boldsymbol{\theta}_0$ (*cf.* Lemma 3.2), and Lemmas 3.6, 3.10, 3.11, and 3.12.

We close this section by mentioning that the assumption (3.4) on the data ϑ, $\boldsymbol{k}$, g, $\boldsymbol{u}_D$, and $\boldsymbol{f}$, which, as shown throughout the foregoing analysis, is a key estimate to derive (3.5), is, unfortunately, unverifiable in practice. In fact, while the data are certainly known in advance, the constants C_4, C_5, C_6, C_7, C_8 involved in that condition (*cf.* (3.12)), which in turn are expressed in terms of the previous constants C_1 and C_2 (*cf.* (3.6)), depend all on boundedness and regularity constants of operators, as well as on parameters, some of which are not explicitly calculable, and hence it is not possible to check whether (3.4) is indeed satisfied or not. This is, however, a quite common fact arising in the analysis of many nonlinear problems, and only in very particular cases (usually related to simple geometries of the domain) it could eventually be circumvented.

3.3 Efficiency

The main result of this section is stated as follows.

Theorem 3.13 *Assume that $\nabla\phi \in \mathrm{L}^4(\Omega)$. Then, there exists a constant $\overline{C}_{\mathtt{eff}} > 0$, which depends only on parameters, $\|\boldsymbol{K}^{-1}\|_\infty$, $|\boldsymbol{k}|$, $\|\boldsymbol{u}_{\mathrm{D}}\|_{1/2,\Gamma_{\mathrm{D}}}$, $\|\boldsymbol{f}\|_{\infty,\Omega}$, $\|\nabla\phi\|_{\mathrm{L}^4(\Omega)}$ and other constants, all them independent of h, such that*

$$\overline{C}_{\mathtt{eff}}\,\boldsymbol{\theta} \leq \|\phi-\phi_h\|_{1,\Omega} + \|\boldsymbol{u}-\boldsymbol{u}_h\|_{1,\Omega} + \|\mathbf{div}(\boldsymbol{\sigma}-\boldsymbol{\sigma}_h)\|_{0,\Omega} + \left\|\frac{1}{\mu(\phi)}\boldsymbol{\sigma}^{\mathtt{d}} - \frac{1}{\mu(\phi_h)}\boldsymbol{\sigma}_h^{\mathtt{d}}\right\|_{0,\Omega} + \text{h.o.t.} \quad (3.36)$$

where h.o.t. *stands for one or several terms of higher order. Moreover, under the assumption that $\boldsymbol{\sigma} \in \mathbb{L}^4(\Omega)$, there exists a constant $C_{\mathtt{eff}} > 0$, which depends only on parameters, $\|\boldsymbol{K}^{-1}\|_\infty$, $|\boldsymbol{k}|$, $\|\boldsymbol{u}_{\mathrm{D}}\|_{1/2,\Gamma_{\mathrm{D}}}$, $\|\boldsymbol{f}\|_{\infty,\Omega}$, $\|\boldsymbol{\sigma}\|_{\mathbb{L}^4(\Omega)}$, $\|\nabla\phi\|_{\mathrm{L}^4(\Omega)}$ and other constants, all them independent of h, such that*

$$C_{\mathtt{eff}}\,\boldsymbol{\theta} \leq \|\phi-\phi_h\|_{1,\Omega} + \|(\boldsymbol{\sigma},\boldsymbol{u}) - (\boldsymbol{\sigma}_h,\boldsymbol{u}_h)\|_H + \text{h.o.t.} \quad (3.37)$$

In the subsequent analysis, such as in [4], we assume for simplicity that the nonlinear functions μ, ϑ, and f_{bk} are such that $\dfrac{1}{\mu(\phi_h)}$, $\vartheta(\phi_h)$, $f_{\mathrm{bk}}(\phi_h)$, and hence $\widetilde{\boldsymbol{\sigma}}_h$ as well, are all piecewise polynomials. In addition, we assume that the data $\boldsymbol{u}_{\mathrm{D}}$ and g are piecewise polynomials. Otherwise, and if μ^{-1}, ϑ, f_{bk}, $\boldsymbol{u}_{\mathrm{D}}$, and g are sufficiently smooth, higher order terms given by the errors arising from suitable polynomial approximations of these expressions and functions would appear in (3.36) and (3.37) (*cf.* Theorem 3.13), which explains the eventual h.o.t. in these expressions. In this regard, and similarly as observed in [4], we remark that (3.36) constitutes a *quasi-efficiency* estimate for the global residual error estimator $\boldsymbol{\theta}$ (*cf.* (3.3)). Indeed, the fact that the expression appearing on the right hand side of (3.36) is not exactly the error, but part of it plus the nonlinear term given by $\|\frac{1}{\mu(\phi)}\boldsymbol{\sigma}^{\mathtt{d}} - \frac{1}{\mu(\phi_h)}\boldsymbol{\sigma}_h^{\mathtt{d}}\|_{0,\Omega}$, explains the *quasi-efficiency* concept employed here. Nevertheless, we show at the end of this section that, under the assumption that $\boldsymbol{\sigma} \in \mathbb{L}^4(\Omega)$, the latter can be bounded by $\|\boldsymbol{\sigma}-\boldsymbol{\sigma}_h\|_{0,\Omega} + \|\phi-\phi_h\|_{1,\Omega}$, thus yielding the efficiency estimate given by (3.37).

In order to prove (3.36) and (3.37), in the rest of this section we derive suitable upper bounds for the ten terms defining the local error indicator θ_T^2 (*cf.* (3.2)). We begin by observing, thanks to the

fact that $\boldsymbol{f}\phi = \boldsymbol{K}^{-1}\boldsymbol{u} - \mathbf{div}\boldsymbol{\sigma}$ in Ω, that there holds

$$\begin{aligned}\|\boldsymbol{f}\phi_h - (\boldsymbol{K}^{-1}\boldsymbol{u}_h - \mathbf{div}\boldsymbol{\sigma}_h)\|_{0,T}^2 \leq 2\,\|\boldsymbol{f}\|_{\infty,\Omega}^2\,\|\phi-\phi_h\|_{0,T}^2 \\ + \quad 4\,\|\boldsymbol{K}^{-1}\|_\infty^2\,\|\boldsymbol{u}-\boldsymbol{u}_h\|_{0,T}^2 + 4\,\|\mathbf{div}(\boldsymbol{\sigma}-\boldsymbol{\sigma}_h)\|_{0,T}^2\,.\end{aligned} \tag{3.38}$$

On the other hand, using that $\nabla\boldsymbol{u} = \frac{1}{\mu(\phi)}\boldsymbol{\sigma}^{\mathtt{d}}$ in Ω, $\boldsymbol{u} = \boldsymbol{u}_{\mathrm{D}}$ on Γ_{D}, and proceeding as in [4, Section 3.3], we deduce that

$$\left\|\nabla\boldsymbol{u}_h - \frac{1}{\mu(\phi_h)}\boldsymbol{\sigma}_h^{\mathtt{d}}\right\|_{0,T}^2 \leq 2\,\|\nabla\boldsymbol{u}-\nabla\boldsymbol{u}_h\|_{0,T}^2 + 2\left\|\frac{1}{\mu(\phi)}\boldsymbol{\sigma}^{\mathtt{d}} - \frac{1}{\mu(\phi_h)}\boldsymbol{\sigma}_h^{\mathtt{d}}\right\|_{0,T}^2 \tag{3.39}$$

and

$$\sum_{e\in\mathcal{E}_h(\Gamma_{\mathrm{D}})}\|\boldsymbol{u}_{\mathrm{D}} - \boldsymbol{u}_h\|_{0,e}^2 \leq c_0^2\,\|\boldsymbol{u}-\boldsymbol{u}_h\|_{1,\Omega}^2\,, \tag{3.40}$$

where c_0 is the norm of the trace operator in $\mathbf{H}^1(\Omega)$.

The efficiency estimates for the remaining seven terms given in (3.3), are provided next. To this end, we proceed as in [11] and [12] (see also [18]), and apply the localization technique (see [34]) based on triangle-bubble and edge-bubble functions, together with extension operators, and inverse inequalities. Therefore, we now introduce further notations and preliminary results. In fact, given $T \in \mathcal{T}_h$ and $e \in \mathcal{E}_h(T)$, we let ψ_T and ψ_e be the usual triangle-bubble and edge-bubble functions, respectively (see [34, eqs. (1.4) and (1.6)]), which satisfy:

i) $\psi_T \in P_3(T)$, $\mathrm{supp}(\psi_T) \subseteq T$, $\psi_T = 0$ on ∂T, and $0 \leq \psi_T \leq 1$ in T.

ii) $\psi_e|_T \in P_2(T)$, $\mathrm{supp}(\psi_e) \subseteq \omega_e := \cup\{T' \in \mathcal{T}_h : e \in \mathcal{E}_h(T')\}$, $\psi_e = 0$ on $\partial T\backslash\{e\}$, and $0 \leq \psi_e \leq 1$ in ω_e.

We also know from [33] that, given $k \in \mathbb{N}\cup\{0\}$, there exists an extension operator $L : C(e) \to C(T)$ that satisfies $L(p) \in P_k(T)$ and $L(p)|_e = p \quad \forall p \in P_k(e)$. A corresponding vectorial version of L, that is the component-wise application of L, is denoted by $\mathbf{L}$. Additional properties of ψ_T, ψ_e and L are collected in the following Lemma.

Lemma 3.14 *Given $k \in \mathbb{N}\cup\{0\}$, there exist positive constants c_1, c_2, c_3, and c_4, depending only on k and the shape regularity of the triangulations (minimum angle condition), such that for each $T \in \mathcal{T}_h$ and $e \in \mathcal{E}_h(T)$, there hold*

$$\begin{aligned}\|\psi_T\,q\|_{0,T}^2 \leq \|q\|_{0,T}^2 \leq c_1\,\|\psi_T^{1/2}\,q\|_{0,T}^2 \qquad \forall\, q \in P_k(T), \\ \|\psi_e\,L(p)\|_{0,T}^2 \leq \|p\|_{0,e}^2 \leq c_2\,\|\psi_e^{1/2}\,p\|_{0,e}^2 \qquad \forall\, p \in P_k(e), \\ c_3\,h_e\,\|p\|_{0,e}^2 \leq \|\psi_e^{1/2}\,L(p)\|_{0,T}^2 \leq c_4\,h_e\,\|p\|_{0,e}^2 \qquad \forall\, p \in P_k(e).\end{aligned} \tag{3.41}$$

Proof. See [33, Lemma 4.1]. □

The following inverse estimate is also required.

Lemma 3.15 *Let $l, m \in \mathbb{N}\cup\{0\}$ such that $l \leq m$. Then, there exists $c > 0$, depending only on k, l, m and the shape regularity of the triangulations, such that for each $T \in \mathcal{T}_h$ there holds*

$$|q|_{m,T} \leq c\,h_T^{l-m}\,|q|_{l,T} \qquad \forall\, q \in P_k(T). \tag{3.42}$$

Proof. See [13, Theorem 3.2.6]. □

In turn, the following lemma, whose proof make use of lemmas 3.14 and 3.15, will be required for the terms involving the **curl** operator and the tangential jumps across the edges of $\mathcal{T}_h$.

Lemma 3.16 *Let $\boldsymbol{\rho}_h \in \mathbb{L}^2(\Omega)$ be a piecewise polynomial of degree $k \geq 0$ on each $T \in \mathcal{T}_h$. In addition, let $\boldsymbol{\rho} \in \mathbb{L}^2(\Omega)$ be such that $\mathbf{curl}(\boldsymbol{\rho}) = 0$ on each $T \in \mathcal{T}_h$. Then, there exist $c, \widetilde{c} > 0$, independent of h, such that*

$$\|\mathbf{curl}(\boldsymbol{\rho}_h)\|_{0,T} \leq c\, h_T^{-1}\, \|\boldsymbol{\rho} - \boldsymbol{\rho}_h\|_{0,T} \qquad \forall\, T \in \mathcal{T}_h$$

and

$$\|[\![\boldsymbol{\rho}_h \boldsymbol{s}_e]\!]\|_{0,e} \leq \widetilde{c}\, h_e^{-1/2}\, \|\boldsymbol{\rho} - \boldsymbol{\rho}_h\|_{0,\omega_e} \qquad \forall\, e \in \mathcal{E}_h\,.$$

Proof. For the first estimate we refer to [11, Lemma 4.3], whereas the second one follows from a slight modification of the proof of [11, Lemma 4.4]. Further details are omitted. □

We now apply Lemma 3.16 to obtain upper bounds for two other terms defining θ_T^2.

Lemma 3.17 *There exist $\widetilde{c}_1, \widetilde{c}_2 > 0$, independent of h such that*

$$h_T^2 \left\| \mathbf{curl}\left\{ \frac{1}{\mu(\phi_h)} \boldsymbol{\sigma}_h^{\mathtt{d}} \right\} \right\|_{0,T}^2 \leq \widetilde{c}_1 \left\| \frac{1}{\mu(\phi)} \boldsymbol{\sigma}^{\mathtt{d}} - \frac{1}{\mu(\phi_h)} \boldsymbol{\sigma}_h^{\mathtt{d}} \right\|_{0,T}^2 \qquad \forall\, T \in \mathcal{T}_h,$$

$$h_e \left\| \left[\!\!\left[\frac{1}{\mu(\phi_h)} \boldsymbol{\sigma}_h^{\mathtt{d}}\, \boldsymbol{s} \right]\!\!\right] \right\|_{0,e}^2 \leq \widetilde{c}_2 \left\| \frac{1}{\mu(\phi)} \boldsymbol{\sigma}^{\mathtt{d}} - \frac{1}{\mu(\phi_h)} \boldsymbol{\sigma}_h^{\mathtt{d}} \right\|_{0,\omega_e}^2 \qquad \forall\, e \in \mathcal{E}_h(\Omega).$$

Proof. It suffices to apply Lemma 3.16 to $\boldsymbol{\rho}_h := \frac{1}{\mu(\phi_h)} \boldsymbol{\sigma}_h^{\mathtt{d}}$ and $\boldsymbol{\rho} := \frac{1}{\mu(\phi)} \boldsymbol{\sigma}^{\mathtt{d}} = \nabla \boldsymbol{u}$. □

Lemma 3.18 *There exists $\widetilde{c}_3 > 0$, independent of h, such that*

$$h_e \left\| \frac{d\boldsymbol{u}_{\mathrm{D}}}{d\boldsymbol{s}} - \frac{1}{\mu(\phi_h)} \boldsymbol{\sigma}_h^{\mathtt{d}}\, \boldsymbol{s} \right\|_{0,e}^2 \leq \widetilde{c}_3 \left\| \frac{1}{\mu(\phi)} \boldsymbol{\sigma}^{\mathtt{d}} - \frac{1}{\mu(\phi_h)} \boldsymbol{\sigma}_h^{\mathtt{d}} \right\|_{0,T_e}^2 \qquad \forall\, e \in \mathcal{E}_h(\Gamma_{\mathrm{D}}).$$

Proof. We proceed similarly as in the proof of [23, Lemma 4.15], by replacing $\mathbf{g}$, Γ, and $\frac{1}{\mu} \boldsymbol{\sigma}_h^{\mathtt{d}}$ in [23] by $\boldsymbol{u}_{\mathrm{D}}$, Γ_{D}, and $\frac{1}{\mu(\phi_h)} \boldsymbol{\sigma}_h^{\mathtt{d}}$, respectively. □

We now aim to provide upper bounds for the three terms completing the definition of the local error indicator θ_T^2 (*cf.* (3.2)). This requires, however, the preliminary result given by the following a priori estimate for the error $\|\widetilde{\boldsymbol{\sigma}} - \widetilde{\boldsymbol{\sigma}}_h\|_{0,T}^2$.

Lemma 3.19 *There exists $C > 0$, depending on ϑ_2, L_f (cf. (2.3), (2.4)), and $|\boldsymbol{k}|$, such that*

$$\|\widetilde{\boldsymbol{\sigma}} - \widetilde{\boldsymbol{\sigma}}_h\|_{0,T}^2 \leq C \left\{ \|\phi - \phi_h\|_{1,T}^2 + \|\boldsymbol{u}(\phi - \phi_h)\|_{0,T}^2 + \|\phi_h(\boldsymbol{u} - \boldsymbol{u}_h)\|_{0,T}^2 + \|(\vartheta(\phi) - \vartheta(\phi_h))\nabla\phi\|_{0,T}^2 \right\}. \quad (3.43)$$

Proof. Employing the definitions of $\widetilde{\boldsymbol{\sigma}}$ (*cf.* (2.1)) and $\widetilde{\boldsymbol{\sigma}}_h$ (*cf.* (3.25)), applying the triangle inequality, and using the Lipschitz continuity assumption on f_{bk} (*cf.* (2.4)), but restricted to each $T \in \mathcal{T}_h$ instead of Ω, we obtain that

$$\begin{aligned} \|\widetilde{\boldsymbol{\sigma}} - \widetilde{\boldsymbol{\sigma}}_h\|_{0,T}^2 \leq 2 \Big\{ & \|\vartheta(\phi)\nabla\phi - \vartheta(\phi_h)\nabla\phi_h\|_{0,T}^2 + 2\, L_f^2\, |\boldsymbol{k}|^2\, \|\phi - \phi_h\|_{0,T}^2 \\ & + 4\, \|\boldsymbol{u}(\phi - \phi_h)\|_{0,T}^2 + 4\, \|\phi_h(\boldsymbol{u} - \boldsymbol{u}_h)\|_{0,T}^2 \Big\}. \end{aligned} \quad (3.44)$$

In turn, applying Cauchy-Schwarz's inequality and the upper bound for ϑ (*cf.* (3.13)), we deduce that

$$\|\vartheta(\phi)\nabla\phi - \vartheta(\phi_h)\nabla\phi_h\|^2_{0,T} \,\leq\, 2\,\|(\vartheta(\phi)-\vartheta(\phi_h))\nabla\phi\|^2_{0,T} \,+\, 2\,\vartheta_2^2\,\|\nabla\phi-\nabla\phi_h\|^2_{0,T}. \tag{3.45}$$

In this way, (3.44) and (3.45) imply (3.43), which finalizes the proof. □

We consider important to remark here that, due to the dependence on ϕ (instead of $|\nabla\phi|$ as in [4]) of the diffusivity ϑ, the first term of our nonlinear operator $A_{\boldsymbol{u}}$ is not necessarily Lipschitz-continuous (as it was the case for the corresponding nonlinear operator in [4, eq. (2.11)]) and hence, in contrast with [4, Lemma 3.19], now the term $\|(\vartheta(\phi)-\vartheta(\phi_h))\nabla\phi\|^2_{0,T}$ appears in the estimate (3.43) of Lemma 3.19. The treatment of such additional term will be postponed to Lemma 3.23.

We now establish the aforementioned efficiency estimates, split into three separate results.

Lemma 3.20 *There exists $\widetilde{c}_4>0$, which depends only on ϑ_2, L_f, β (cf. (2.3), (2.4), (2.1)), $|\boldsymbol{k}|$, and other constants, all them independent of h, such that*

$$\begin{aligned} h_T^2\,\|g\,-\,(\beta\phi_h\,-\,\mathrm{div}\,\widetilde{\boldsymbol{\sigma}}_h)\|^2_{0,T} \,\leq\, \widetilde{c}_4\,\Big\{&\|\phi-\phi_h\|^2_{1,T}\,+\,\|\boldsymbol{u}(\phi-\phi_h)\|^2_{0,T} \\ &+\|\phi_h(\boldsymbol{u}-\boldsymbol{u}_h)\|^2_{0,T}\,+\,\|(\vartheta(\phi)-\vartheta(\phi_h))\nabla\phi\|^2_{0,T}\,+\,h_T^2\,\|\phi-\phi_h\|^2_{0,T}\Big\}. \end{aligned} \tag{3.46}$$

Proof. It is an adaptation of the proof of [4, Lemma 3.22]. Indeed, given $T\in\mathcal{T}_h$, using the properties (3.41), the fact that $\beta\phi-\mathrm{div}\,\widetilde{\boldsymbol{\sigma}}\,=\,g$ in Ω, and integrating by parts, we deduce that

$$\begin{aligned} &\|g-(\beta\phi_h-\mathrm{div}\,\widetilde{\boldsymbol{\sigma}}_h)\|^2_{0,T} \,\leq\, c_1\,\|\psi_T^{1/2}\,(g-(\beta\phi_h-\mathrm{div}\,\widetilde{\boldsymbol{\sigma}}_h))\|^2_{0,T} \\ &=\,-c_1\int_T\nabla\big(\psi_T\,(g-(\beta\phi_h-\mathrm{div}\,\widetilde{\boldsymbol{\sigma}}_h)\big)\cdot(\widetilde{\boldsymbol{\sigma}}-\widetilde{\boldsymbol{\sigma}}_h)\,+\,c_1\,\beta\int_T\psi_T\,(g-(\beta\phi_h-\mathrm{div}\,\widetilde{\boldsymbol{\sigma}}_h))\,(\phi-\phi_h). \end{aligned}$$

Then, the Cauchy-Schwarz inequality, the inverse estimate (3.42), the fact that $0\leq\psi_T\leq 1$, and the triangle inequality imply that

$$\begin{aligned} \|g-(\beta\phi_h-\mathrm{div}\,\widetilde{\boldsymbol{\sigma}}_h)\|^2_{0,T} \,\leq\, &c_1\,c\,h_T^{-1}\|g-(\beta\phi_h-\mathrm{div}\,\widetilde{\boldsymbol{\sigma}}_h)\|_{0,T}\,\|\widetilde{\boldsymbol{\sigma}}-\widetilde{\boldsymbol{\sigma}}_h\|_{0,T} \\ &+\quad c_1\beta\,\|g-(\beta\phi_h-\mathrm{div}\,\widetilde{\boldsymbol{\sigma}}_h)\|_{0,T}\,\|\phi-\phi_h\|_{0,T}\,, \end{aligned}$$

which gives

$$h_T\|g-(\beta\phi_h-\mathrm{div}\,\widetilde{\boldsymbol{\sigma}}_h)\|_{0,T} \,\leq\, C\,\Big\{\|\widetilde{\boldsymbol{\sigma}}-\widetilde{\boldsymbol{\sigma}}_h\|_{0,T}\,+\,h_T\,\|\phi-\phi_h\|_{0,T}\Big\}.$$

The foregoing inequality together with (3.43) imply (3.46), and thus the proof is completed. □

Lemma 3.21 *There exists $\widetilde{c}_5>0$, which depends only on ϑ_2, L_f, β (cf. (2.3), (2.4), (2.1)), $|\boldsymbol{k}|$, and other constants, all them independent of h, such that for each $e\in\mathcal{E}_h(\Omega)$ there holds*

$$\begin{aligned} h_e\,\|[\![\widetilde{\boldsymbol{\sigma}}_h\cdot\boldsymbol{\nu}_e]\!]\|^2_{0,e} \,\leq\, \widetilde{c}_5\sum_{T\subseteq\omega_e}\Big\{&\|\phi-\phi_h\|^2_{1,T}\,+\,\|\boldsymbol{u}(\phi-\phi_h)\|^2_{0,T}\,+\,\|\phi_h(\boldsymbol{u}-\boldsymbol{u}_h)\|^2_{0,T} \\ &+\quad\|(\vartheta(\phi)-\vartheta(\phi_h))\nabla\phi\|^2_{0,T}\,+\,h_T^2\,\|\phi-\phi_h\|^2_{0,T}\Big\}, \end{aligned}$$

where ω_e is the union of the two triangles in $\mathcal{T}_h$ having e as an edge.

Proof. See [4, Lemma 3.21]. □

Lemma 3.22 *There exists $\widetilde{c}_6 > 0$, which depends only on ϑ_2, L_f, β (cf. (2.3), (2.4), (2.1)), $|\boldsymbol{k}|$, and other constants, all them independent of h, such that for each $e \in \mathcal{E}_h(\Gamma_{\rm N})$ there holds*

$$h_e \, \|\widetilde{\boldsymbol{\sigma}}_h \cdot \boldsymbol{\nu}\|^2_{0,e} \leq \widetilde{c}_6 \Big\{ \|\phi - \phi_h\|^2_{1,T} + \|\boldsymbol{u}(\phi - \phi_h)\|^2_{0,T} + \|\phi_h(\boldsymbol{u} - \boldsymbol{u}_h)\|^2_{0,T} + \|(\vartheta(\phi) - \vartheta(\phi_h))\nabla\phi\|^2_{0,T} + h_T^2 \, \|\phi - \phi_h\|^2_{0,T} \Big\},$$

where T is the triangle of $\mathcal{T}_h$ having e as an edge.

Proof. See [4, Lemma 3.22]. □

In order to complete the proof of global efficiency given by (3.36), it only remains to estimate properly the three terms: $\|\boldsymbol{u}(\phi - \phi_h)\|^2_{0,T}$, $\|\phi_h(\boldsymbol{u} - \boldsymbol{u}_h)\|^2_{0,T}$ and $\|(\vartheta(\phi) - \vartheta(\phi_h))\nabla\phi\|^2_{0,T}$, appearing in the upper bounds provided by the last four lemmas, which is indeed the purpose of the following lemma.

Lemma 3.23 *There exist positive constants $\widetilde{c}_7, \widetilde{c}_8$, independent of h, such that*

$$\sum_{T \in \mathcal{T}_h} \|\boldsymbol{u}\,(\phi - \phi_h)\|^2_{0,T} \leq \widetilde{c}_7 \, \|\phi - \phi_h\|^2_{1,\Omega} \quad \text{and} \quad \sum_{T \in \mathcal{T}_h} \|\phi_h(\boldsymbol{u} - \boldsymbol{u}_h)\|^2_{0,T} \leq \widetilde{c}_8 \, \|\boldsymbol{u} - \boldsymbol{u}_h\|^2_{1,\Omega}, \tag{3.47}$$

where $\widetilde{c}_7$ depends on $\|\boldsymbol{u}_{\rm D}\|_{1/2,\Gamma_{\rm D}}$, $\|\boldsymbol{f}\|_{\infty,\Omega}$ and r (cf. (3.1)), and $\widetilde{c}_8$ depends on r. In addition, assuming $\nabla\phi \in \mathrm{L}^4(\Omega)$, there exists a positive constant $\widetilde{c}_9$, independent of h, such that

$$\sum_{T \in \mathcal{T}_h} \|(\vartheta(\phi) - \vartheta(\phi_h))\nabla\phi\|^2_{0,T} \leq \widetilde{c}_9 \, \|\phi - \phi_h\|^2_{1,\Omega}\,, \tag{3.48}$$

where $\widetilde{c}_9$ depends on L_ϑ (cf. (2.4)) and $\|\nabla\phi\|_{\mathrm{L}^4(\Omega)}$.

Proof. The estimates given in (3.47) were established in [4, eq. (3.71)-(3.72)]. On the other hand, using the Lipschitz continuity assumption on ϑ (*cf.* (2.4)), but restricted to each triangle $T \in \mathcal{T}_h$ instead of Ω, employing Cauchy-Schwarz's inequality and the compactness (and hence continuity) of the injection $i : \mathrm{H}^1(\Omega) \to \mathrm{L}^4(\Omega)$ (*cf.* [1, Theorem 6.3], [28, Theorem 1.3.5]), we deduce that

$$\begin{aligned} \sum_{T \in \mathcal{T}_h} \|(\vartheta(\phi) - \vartheta(\phi_h))\nabla\phi\|^2_{0,T} &\leq \sum_{T \in \mathcal{T}_h} L_\vartheta^2 \, \|\phi - \phi_h\|^2_{\mathrm{L}^4(T)} \, \|\nabla\phi\|^2_{\mathrm{L}^4(T)} \\ &\leq L_\vartheta^2 \, \|\phi - \phi_h\|^2_{\mathrm{L}^4(\Omega)} \, \|\nabla\phi\|^2_{\mathrm{L}^4(\Omega)} \leq \widetilde{c}_9 \, \|\phi - \phi_h\|^2_{1,\Omega}\,, \end{aligned}$$

where $\widetilde{c}_9$ depends only on $\|i\|$, L_ϑ, and $\|\nabla\phi\|_{\mathrm{L}^4(\Omega)}$, which gives (3.48) and finishes the proof. □

By virtue of the estimates (3.38), (3.39), (3.40), Lemmas 3.17, 3.18, 3.20, 3.21, and 3.22, and the final estimates given by (3.47) and (3.48), we deduce (3.36). Finally, assuming now that $\boldsymbol{\sigma} \in \mathbb{L}^4(\Omega)$ and proceeding as at the end of the proof of [4, Theorem 3.13], we find that

$$\left\| \frac{1}{\mu(\phi)} \boldsymbol{\sigma}^{\mathtt{d}} - \frac{1}{\mu(\phi_h)} \boldsymbol{\sigma}_h^{\mathtt{d}} \right\|_{0,\Omega} \leq C \Big\{ \|\boldsymbol{\sigma} - \boldsymbol{\sigma}_h\|_{0,\Omega} + \|\phi - \phi_h\|_{1,\Omega} \Big\}, \tag{3.49}$$

where C is a positive constant, independent of h, that depends only on μ_1 (*cf.* (2.3)), L_μ (*cf.* (2.4)) and $\|\boldsymbol{\sigma}\|_{\mathbb{L}^4(\Omega)}$. In this way, combining (3.49) and (3.36), we arrive at (3.37), which completes the proof of Theorem 3.13.

4 A second residual-based a posteriori error estimator

In this section we derive another *a posteriori* error estimator for our augmented mixed-primal finite element scheme (2.8), with the same discrete spaces introduced in the Section 2.3. In turn, the reliability of our new estimator can be proved without resorting to Helmholtz decompositions. More precisely, this second estimator arises simply employing the alternative definition of the functional E_h (*cf.* (3.11)) and bounding $\|E_h\|_{\mathbb{H}_N(\mathbf{div},\Omega)'}$ in the preliminary estimate for the total error given by (3.24) (*cf.* Theorem 3.4). Then, with the same notations and discrete spaces introduced in Sections 2 and 3, we now set for each $T \in \mathcal{T}_h$ the local error indicator

$$\begin{aligned}\widetilde{\theta}_T^2 \,:=\, &\|\boldsymbol{f}\phi_h \,-\, (\boldsymbol{K}^{-1}\boldsymbol{u}_h \,-\, \mathbf{div}\boldsymbol{\sigma}_h)\|_{0,T}^2 \,+\, \left\|\nabla \boldsymbol{u}_h \,-\, \frac{1}{\mu(\phi_h)}\boldsymbol{\sigma}_h^{\mathtt{d}}\right\|_{0,T}^2 \,+\, h_T^2\,\|g \,-\, (\beta\phi_h \,-\, \mathrm{div}\,\widetilde{\boldsymbol{\sigma}}_h)\|_{0,T}^2 \\ &+ \sum_{e\in\mathcal{E}_h(T)\cap\mathcal{E}_h(\Omega)} h_e\,\|[\![\widetilde{\boldsymbol{\sigma}}_h\cdot\boldsymbol{\nu}_e]\!]\|_{0,e}^2 \,+\, \sum_{e\in\mathcal{E}_h(T)\cap\mathcal{E}_h(\Gamma_{\mathrm{N}})} h_e\,\|\widetilde{\boldsymbol{\sigma}}_h\cdot\boldsymbol{\nu}\|_{0,e}^2 \,+\, \sum_{e\in\mathcal{E}_h(T)\cap\mathcal{E}_h(\Gamma_{\mathrm{D}})} \|\boldsymbol{u}_{\mathrm{D}} - \boldsymbol{u}_h\|_{0,e}^2\,,\end{aligned} \tag{4.1}$$

and define the following global residual error estimator

$$\widetilde{\boldsymbol{\theta}}^{\,2} \,:=\, \sum_{T\in\mathcal{T}_h} \widetilde{\theta}_T^2 \,+\, \|\boldsymbol{u}_{\mathrm{D}} - \boldsymbol{u}_h\|_{1/2,\Gamma_{\mathrm{D}}}^2\,. \tag{4.2}$$

Throughout the rest of this section, we establish *quasi-local* reliability and efficiency for the estimator $\widetilde{\boldsymbol{\theta}}$. The name *quasi-local* refers here to the fact that the last term defining $\widetilde{\boldsymbol{\theta}}$ can not be decomposed into local quantities associated to each triangle $T \in \mathcal{T}_h$ (unless it is either conveniently bounded or previously modified, as we will see below).

Theorem 4.1 *Assume that the data $\boldsymbol{k}$, g, ϑ, $\boldsymbol{u}_{\mathrm{D}}$, and $\boldsymbol{f}$ are sufficiently small so that there holds*

$$C_4\,|\boldsymbol{k}| \,+\, C_5\,\|g\|_{\delta,\Omega} \,+\, C_6\,\vartheta_2 \,+\, C_7\,\|\boldsymbol{u}_{\mathrm{D}}\|_{1/2+\delta,\Gamma_{\mathrm{D}}} \,+\, C_8\,\|\boldsymbol{f}\|_{\infty,\Omega} \,<\, \frac{1}{2},$$

where C_4, C_5, C_6, C_7 and C_8 are the constants given in (3.12). Then, there exists a constant $\widetilde{C}_{\mathtt{rel}} > 0$, which depends only on $\|\boldsymbol{u}_{\mathrm{D}}\|_{1/2+\delta,\Gamma_{\mathrm{D}}}$, $\|\boldsymbol{f}\|_{\infty,\Omega}$ and other constants, all them independent of h, such that

$$\|\phi - \phi_h\|_{1,\Omega}^2 \,+\, \|(\boldsymbol{\sigma},\boldsymbol{u}) - (\boldsymbol{\sigma}_h,\boldsymbol{u}_h)\|_H^2 \,\leq\, \widetilde{C}_{\mathtt{rel}}\,\widetilde{\boldsymbol{\theta}}^{\,2}\,. \tag{4.3}$$

Proof. Using the alternative definition of the functional E_h (*cf.* (3.11)), and then applying the Cauchy-Schwarz inequality, we deduce that

$$\begin{aligned}\|E_h\|_{\mathbb{H}_N(\mathbf{div},\Omega)'} \,\leq\, C\,\Big\{&\|\boldsymbol{u}_{\mathrm{D}} \,-\, \boldsymbol{u}_h\|_{1/2,\Gamma_{\mathrm{D}}} \,+\, \left\|\nabla\boldsymbol{u}_h \,-\, \frac{1}{\mu(\phi_h)}\boldsymbol{\sigma}_h^{\mathtt{d}}\right\|_{0,\Omega} \\ &+\, \|\boldsymbol{f}\phi_h \,-\, (\boldsymbol{K}^{-1}\boldsymbol{u}_h \,-\, \mathbf{div}\boldsymbol{\sigma}_h)\|_{0,\Omega}\Big\}\,,\end{aligned} \tag{4.4}$$

where C is a positive constant independent of h. Then, replacing (4.4) back into (3.24) (*cf.* Theorem 3.4), and employing again the upper bound for $\|\widetilde{E}_h\|_{\mathrm{H}^1_{\Gamma_{\mathrm{D}}}(\Omega)'}$ (*cf.* Lemma 3.6), and the definition of $\boldsymbol{\theta}_0$ (*cf.* Lemma 3.2), we obtain (4.3) and finish the proof. □

Theorem 4.2 *Assume that $\nabla\phi \in \mathrm{L}^4(\Omega)$. Then, there exists a constant $C^*_{\mathtt{eff}} > 0$, which depends only on parameters, $\|\boldsymbol{K}^{-1}\|_\infty$, $|\boldsymbol{k}|$, $\|\boldsymbol{u}_{\mathrm{D}}\|_{1/2,\Gamma_{\mathrm{D}}}$, $\|\boldsymbol{f}\|_{\infty,\Omega}$, $\|\nabla\phi\|_{\mathrm{L}^4(\Omega)}$, and other constants, all them independent of h, such that*

$$C^*_{\mathtt{eff}}\,\widetilde{\boldsymbol{\theta}}^{\,2} \,\leq\, \|\phi-\phi_h\|_{1,\Omega}^2 + \|\boldsymbol{u}-\boldsymbol{u}_h\|_{1,\Omega}^2 + \|\mathbf{div}(\boldsymbol{\sigma}-\boldsymbol{\sigma}_h)\|_{0,\Omega}^2 + \left\|\frac{1}{\mu(\phi)}\boldsymbol{\sigma}^{\mathtt{d}} - \frac{1}{\mu(\phi_h)}\boldsymbol{\sigma}_h^{\mathtt{d}}\right\|_{0,\Omega}^2 + \text{h.o.t.} \tag{4.5}$$

where h.o.t. *stands for one or several terms of higher order. Moreover, assuming* $\boldsymbol{\sigma} \in \mathbb{L}^4(\Omega)$*, there exists a constant* $\widetilde{C}_{\mathtt{eff}} > 0$*, which depends only on parameters,* $\|\boldsymbol{K}^{-1}\|_\infty$*,* $|\boldsymbol{k}|$*,* $\|\boldsymbol{u}_{\mathrm{D}}\|_{1/2,\Gamma_{\mathrm{D}}}$*,* $\|\boldsymbol{f}\|_{\infty,\Omega}$*,* $\|\nabla\phi\|_{\mathrm{L}^4(\Omega)}$*,* $\|\boldsymbol{\sigma}\|_{\mathbb{L}^4(\Omega)}$*, and other constants, all them independent of* h*, such that*

$$\widetilde{C}_{\mathtt{eff}}\,\widetilde{\boldsymbol{\theta}}^2 \,\leq\, \|\phi - \phi_h\|^2_{1,\Omega} \,+\, \|(\boldsymbol{\sigma},\boldsymbol{u}) - (\boldsymbol{\sigma}_h,\boldsymbol{u}_h)\|^2_H \,+\, \text{h.o.t.} \tag{4.6}$$

Proof. We proceed as in the proof of [4, Theorem 4.2]. In fact, thanks to the trace theorem in $\mathbf{H}^1(\Omega)$, there exists $c > 0$, depending on Γ_{D} and Ω, such that

$$\|\boldsymbol{u}_{\mathrm{D}} - \boldsymbol{u}_h\|^2_{1/2,\Gamma_{\mathrm{D}}} \,\leq\, c\,\|\boldsymbol{u} - \boldsymbol{u}_h\|^2_{1,\Omega}\,.$$

Next, the estimates (4.5) and (4.6) are obtained by applying the same arguments employed in the proof of Theorem 3.13 (*cf.* Section 3.3), and hence we omit further details. □

We point out here that, in order to use the indicator $\widetilde{\boldsymbol{\theta}}$ (*cf.* (4.2)) in an adaptive algorithm that solves (2.8), we need to estimate the expression $\|\boldsymbol{u}_{\mathrm{D}} - \boldsymbol{u}_h\|^2_{1/2,\Gamma_{\mathrm{D}}}$ through local terms. To this end, as well as in [4], we now employ an interpolation argument and replace the aforementioned expression by a suitable upper bound, which yields a reliable and fully local *a posteriori* error estimate.

Theorem 4.3 *Assume that the data* $\boldsymbol{k}$*,* g*,* ϑ*,* $\boldsymbol{u}_{\mathrm{D}}$*, and* $\boldsymbol{f}$ *are sufficiently small so that there holds*

$$C_4\,|\boldsymbol{k}| \,+\, C_5\,\|g\|_{\delta,\Omega} \,+\, C_6\,\vartheta_2 \,+\, C_7\,\|\boldsymbol{u}_{\mathrm{D}}\|_{1/2+\delta,\Gamma_{\mathrm{D}}} \,+\, C_8\,\|\boldsymbol{f}\|_{\infty,\Omega} \,<\, \frac{1}{2},$$

where C_4*,* C_5*,* C_6*,* C_7 *and* C_8 *are the constants given in* (3.12) *In turn, let* $\widehat{\boldsymbol{\theta}}^2 := \displaystyle\sum_{T\in\mathcal{T}_h} \widehat{\theta}^2_T$*, where for each* $T \in \mathcal{T}_h$ *we set*

$$\widehat{\theta}^2_T \,:=\, \|\boldsymbol{f}\phi_h \,-\, (\boldsymbol{K}^{-1}\boldsymbol{u}_h \,-\, \mathbf{div}\boldsymbol{\sigma}_h)\|^2_{0,T} \,+\, \left\|\nabla\boldsymbol{u}_h \,-\, \frac{1}{\mu(\phi_h)}\boldsymbol{\sigma}^{\mathtt{d}}_h\right\|^2_{0,T} \,+\, h^2_T\,\|g \,-\, (\beta\phi_h \,-\, \operatorname{div}\widetilde{\boldsymbol{\sigma}}_h)\|^2_{0,T}$$
$$+ \sum_{e\in\mathcal{E}_h(T)\cap\mathcal{E}_h(\Omega)} h_e\,\|[\![\widetilde{\boldsymbol{\sigma}}_h\cdot\boldsymbol{\nu}_e]\!]\|^2_{0,e} \,+\, \sum_{e\in\mathcal{E}_h(T)\cap\mathcal{E}_h(\Gamma_{\mathrm{N}})} h_e\,\|\widetilde{\boldsymbol{\sigma}}_h\cdot\boldsymbol{\nu}\|^2_{0,e} \,+\, \sum_{e\in\mathcal{E}_h(T)\cap\mathcal{E}_h(\Gamma_{\mathrm{D}})} \|\boldsymbol{u}_{\mathrm{D}} - \boldsymbol{u}_h\|^2_{1,e}\,.$$

Then, there exists a constant $\widehat{C}_{\mathtt{rel}} > 0$*, which depends only on parameters,* $\|\boldsymbol{u}_{\mathrm{D}}\|_{1/2+\delta,\Gamma_{\mathrm{D}}}$*,* $\|\boldsymbol{f}\|_{\infty,\Omega}$ *and other constants, all them independent of* h*, such that*

$$\|\phi - \phi_h\|^2_{1,\Omega} \,+\, \|(\boldsymbol{\sigma},\boldsymbol{u}) - (\boldsymbol{\sigma}_h,\boldsymbol{u}_h)\|^2_H \,\leq\, \widehat{C}_{\mathtt{rel}}\,\widehat{\boldsymbol{\theta}}^2\,.$$

Proof. The proof reduces to bound the term $\|\boldsymbol{u}_{\mathrm{D}} - \boldsymbol{u}_h\|_{1/2,\Gamma_{\mathrm{D}}}$. To this end, it suffices to apply the fact that $H^{1/2}(\Gamma_{\mathrm{D}})$ is the interpolation space with index $1/2$ between $H^1(\Gamma_{\mathrm{D}})$ and $L^2(\Gamma_{\mathrm{D}})$, and proceed as in [4, Theorem 4.3]. □

5 Residual-based a posteriori error estimators: The 3D case

In this section we extend the results from Sections 3 and 4 to the three-dimensional version of (2.8). Analogously, as in Section 3, given a tetrahedron $T \in \mathcal{T}_h$, we let $\mathcal{E}_h(T)$ be the set of its faces, and let $\mathcal{E}_h$ be the set of all faces of the triangulation $\mathcal{T}_h$. Then, we write $\mathcal{E}_h = \mathcal{E}_h(\Omega) \cup \mathcal{E}_h(\Gamma)$, where $\mathcal{E}_h(\Omega) := \{e \in \mathcal{E}_h : e \subseteq \Omega\}$ and $\mathcal{E}_h(\Gamma) := \{e \in \mathcal{E}_h : e \subseteq \Gamma\}$. Also, for each face $e \in \mathcal{E}_h$ we fix a unit normal $\boldsymbol{\nu}_e$ to e, so that given $\boldsymbol{\tau} \in \mathbb{L}^2(\Omega)$ such that $\boldsymbol{\tau}|_T \in \mathbb{C}(T)$ on each $T \in \mathcal{T}_h$, and given $e \in \mathcal{E}_h(\Omega)$, we let $[\![\boldsymbol{\tau}\times\boldsymbol{\nu}_e]\!]$ be the corresponding jump of the tangential traces across e, that is

$[\![\boldsymbol{\tau}\times\boldsymbol{\nu}_e]\!] := (\boldsymbol{\tau}|_T - \boldsymbol{\tau}|_{T'})|_e \times \boldsymbol{\nu}_e$, where T and T' are the elements of $\mathcal{T}_h$ having e as a common face. In what follows, when no confusion arises, we simple write $\boldsymbol{\nu}$ instead of $\boldsymbol{\nu}_e$.

Now, we recall that the curl of a 3D vector $\boldsymbol{v} := (v_1, v_2, v_3)$ is the 3D vector

$$\mathrm{curl}(\boldsymbol{v}) \;=\; \nabla\times\boldsymbol{v} \;:=\; \left(\frac{\partial v_3}{\partial x_2} - \frac{\partial v_2}{\partial x_3}, \frac{\partial v_1}{\partial x_3} - \frac{\partial v_3}{\partial x_1}, \frac{\partial v_2}{\partial x_1} - \frac{\partial v_1}{\partial x_2}\right),$$

and that, given a tensor function $\boldsymbol{\tau} := (\tau_{ij})_{3\times 3}$, the operator **curl** denotes curl acting along each row of $\boldsymbol{\tau}$, and $\boldsymbol{\tau}\times\boldsymbol{\nu}$ is a tensor whose rows are the tangential components of each row of $\boldsymbol{\tau}$, that is,

$$\mathbf{curl}(\boldsymbol{\tau}) \;:=\; \begin{pmatrix} \mathrm{curl}(\tau_{11},\tau_{12},\tau_{13}) \\ \mathrm{curl}(\tau_{21},\tau_{22},\tau_{23}) \\ \mathrm{curl}(\tau_{31},\tau_{32},\tau_{33}) \end{pmatrix}, \quad \text{and} \quad \boldsymbol{\tau}\times\boldsymbol{\nu} \;:=\; \begin{pmatrix} (\tau_{11},\tau_{12},\tau_{13})\times\boldsymbol{\nu} \\ (\tau_{21},\tau_{22},\tau_{23})\times\boldsymbol{\nu} \\ (\tau_{31},\tau_{32},\tau_{33})\times\boldsymbol{\nu} \end{pmatrix}.$$

We now set for each $T\in\mathcal{T}_h$ the local *a posteriori* error indicator θ_T^2 as follows

$$\begin{aligned}
\theta_T^2 :=& \|\boldsymbol{f}\phi_h - (\boldsymbol{K}^{-1}\boldsymbol{u}_h - \mathbf{div}\boldsymbol{\sigma}_h)\|_{0,T}^2 + \left\|\nabla\boldsymbol{u}_h - \frac{1}{\mu(\phi_h)}\boldsymbol{\sigma}_h^{\mathtt{d}}\right\|_{0,T}^2 + h_T^2\,\|g - (\beta\phi_h - \operatorname{div}\widetilde{\boldsymbol{\sigma}}_h)\|_{0,T}^2 \\
&+ h_T^2\left\|\mathbf{curl}\left\{\frac{1}{\mu(\phi_h)}\boldsymbol{\sigma}_h^{\mathtt{d}}\right\}\right\|_{0,T}^2 + \sum_{e\in\mathcal{E}_h(T)\cap\mathcal{E}_h(\Omega)} h_e\left\|\left[\!\left[\frac{1}{\mu(\phi_h)}\boldsymbol{\sigma}_h^{\mathtt{d}}\times\boldsymbol{\nu}\right]\!\right]\right\|_{0,e}^2 \\
&+ \sum_{e\in\mathcal{E}_h(T)\cap\mathcal{E}_h(\Omega)} h_e\,\|[\![\widetilde{\boldsymbol{\sigma}}_h\cdot\boldsymbol{\nu}_e]\!]\|_{0,e}^2 + \sum_{e\in\mathcal{E}_h(T)\cap\mathcal{E}_h(\Gamma_{\mathrm{N}})} h_e\,\|\widetilde{\boldsymbol{\sigma}}_h\cdot\boldsymbol{\nu}\|_{0,e}^2 \\
&+ \sum_{e\in\mathcal{E}_h(T)\cap\mathcal{E}_h(\Gamma_{\mathrm{D}})} \|\boldsymbol{u}_{\mathrm{D}} - \boldsymbol{u}_h\|_{0,e}^2 + \sum_{e\in\mathcal{E}_h(T)\cap\mathcal{E}_h(\Gamma_{\mathrm{D}})} h_e\left\|\nabla\boldsymbol{u}_{\mathrm{D}}\times\boldsymbol{\nu} - \frac{1}{\mu(\phi_h)}\boldsymbol{\sigma}_h^{\mathtt{d}}\times\boldsymbol{\nu}\right\|_{0,e}^2,
\end{aligned} \tag{5.1}$$

whereas $\widetilde{\theta}_T^2$ stays exactly as in (4.1). In this way, the corresponding global *a posteriori* error estimators are defined as (3.3) and (4.2), that is

$$\boldsymbol{\theta}^2 \;:=\; \sum_{T\in\mathcal{T}_h}\theta_T^2 \quad\text{and}\quad \widetilde{\boldsymbol{\theta}}^2 \;:=\; \sum_{T\in\mathcal{T}_h}\widetilde{\theta}_T^2 \;+\; \|\boldsymbol{u}_{\mathrm{D}} - \boldsymbol{u}_h\|_{1/2,\Gamma_{\mathrm{D}}}^2.$$

We now establish the analogue of Theorems 3.1 and 4.1, respectively.

Theorem 5.1 (Reliability of $\boldsymbol{\theta}$) *Assume that Ω is a connected domain and that Γ_{N} is the boundary of a convex extension of Ω. In addition, assume that the data $\boldsymbol{k}$, g, ϑ, $\boldsymbol{u}_{\mathrm{D}}$, and $\boldsymbol{f}$ are sufficiently small so that there holds*

$$C_4\,|\boldsymbol{k}| \;+\; C_5\,\|g\|_{\delta,\Omega} \;+\; C_6\,\vartheta_2 \;+\; C_7\,\|\boldsymbol{u}_{\mathrm{D}}\|_{1/2+\delta,\Gamma_{\mathrm{D}}} \;+\; C_8\,\|\boldsymbol{f}\|_{\infty,\Omega} \;<\; \frac{1}{2},$$

where C_4, C_5, C_6, C_7 and C_8 are the constants given below in (3.12). Then, there exists a constant $C_{\mathtt{rel}} > 0$, which depends only on parameters, $\|\boldsymbol{u}_{\mathrm{D}}\|_{1/2+\delta,\Gamma_{\mathrm{D}}}$, $\|\boldsymbol{f}\|_{\infty,\Omega}$, and other constants, all them independent of h, such that

$$\|\phi - \phi_h\|_{1,\Omega} \;+\; \|(\boldsymbol{\sigma},\boldsymbol{u}) - (\boldsymbol{\sigma}_h,\boldsymbol{u}_h)\|_H \;\leq\; C_{\mathtt{rel}}\,\boldsymbol{\theta}.$$

The proof of Theorem 5.1 follows from a very similar analysis to the Section 3.2, except in a few points to be described throughout the following discussion. Indeed, we first need to use a 3D version of the stable Helmholtz decomposition, provided by Lemma 3.7, which was established recently in [20, Theorem 3.2]. We remark that the proof of [20, Theorem 3.2] makes use of several estimates available in [2] and combines similar arguments to those from the proofs of [20, Theorem 3.1] and [4, Lemma 3.9]. Then, the associated discrete Helmholtz decomposition and the functional E_h are set and rewritten exactly as in (3.30) and (3.31), respectively. Secondly, in order to derive the upper bound to $\|E_h\|_{\mathbb{H}_N(\mathbf{div},\Omega)'}$, we need to employ the 3D analogue of the integration by parts formula on the boundary given by (3.32) (*cf.* Lemma 3.9). In fact, by employing the identities from [25, Chapter I, eq. (2.17) and Theorem 2.11], we find that in the 3D case, there holds

$$\langle \underline{\mathbf{curl}}\, \boldsymbol{\chi}\, \boldsymbol{\nu}, \boldsymbol{\phi} \rangle \;=\; -\langle \nabla \boldsymbol{\phi} \times \boldsymbol{\nu}, \boldsymbol{\chi} \rangle \qquad \forall\, \boldsymbol{\chi} \in \mathbb{H}^1(\Omega), \quad \forall\, \boldsymbol{\phi} \in \mathbf{H}^1(\Omega). \tag{5.2}$$

On the other hand, the integration by parts formula on each tetrahedron $T \in \mathcal{T}_h$, which is employed in the proof of the 3D analogue of Lemma 3.10 (see also [4, Lemma 3.11]), becomes (*cf.* [25, Chapter I, Theorem 2.11])

$$\int_T \underline{\mathbf{curl}}\, \boldsymbol{\tau} : \boldsymbol{\chi} \;-\; \int_T \boldsymbol{\tau} : \underline{\mathbf{curl}}\, \boldsymbol{\chi} \;=\; \langle \boldsymbol{\tau} \times \boldsymbol{\nu}, \boldsymbol{\chi} \rangle_{\partial T} \qquad \forall\, \boldsymbol{\tau} \in \mathbb{H}(\underline{\mathbf{curl}}; \Omega), \qquad \forall\, \boldsymbol{\chi} \in \mathbb{H}^1(\Omega), \tag{5.3}$$

where $\langle \cdot, \cdot \rangle_{\partial T}$ is the duality pairing between $\mathbb{H}^{-1/2}(T)$ and $\mathbb{H}^{1/2}(T)$, and, as usual, $\mathbb{H}(\underline{\mathbf{curl}}; \Omega)$ corresponds to the space of tensors in $\mathbb{L}^2(\Omega)$ whose $\underline{\mathbf{curl}}$ belongs to $\mathbb{L}^2(\Omega)$. Notice that the identities (5.2) and (5.3) explain the appearing of the expressions $\dfrac{1}{\mu(\phi_h)} \boldsymbol{\sigma}_h^{\mathtt{d}} \times \boldsymbol{\nu}$ and $\nabla \boldsymbol{u}_{\mathrm{D}} \times \boldsymbol{\nu} - \dfrac{1}{\mu(\phi_h)} \boldsymbol{\sigma}_h^{\mathtt{d}} \times \boldsymbol{\nu}$ in the 3D definition of $\boldsymbol{\theta}$ (*cf.* (5.1)).

Theorem 5.2 (Reliability of $\widetilde{\boldsymbol{\theta}}$) *Assume that the data $\boldsymbol{k}$, g, ϑ, $\boldsymbol{u}_{\mathrm{D}}$, and $\boldsymbol{f}$ are sufficiently small so that there holds*

$$C_4\, |\boldsymbol{k}| \;+\; C_5\, \|g\|_{\delta,\Omega} \;+\; C_6\, \vartheta_2 \;+\; C_7\, \|\boldsymbol{u}_{\mathrm{D}}\|_{1/2+\delta,\Gamma_{\mathrm{D}}} \;+\; C_8\, \|\boldsymbol{f}\|_{\infty,\Omega} \;<\; \frac{1}{2},$$

where C_4, C_5, C_6, C_7 and C_8 are the constants given in (3.12). Then, there exists a constant $\widetilde{C}_{\mathtt{rel}} > 0$, which depends only on $\|\boldsymbol{u}_{\mathrm{D}}\|_{1/2+\delta,\Gamma_{\mathrm{D}}}$, $\|\boldsymbol{f}\|_{\infty,\Omega}$ and other constants, all them independent of h, such that

$$\|\phi - \phi_h\|_{1,\Omega}^2 \;+\; \|(\boldsymbol{\sigma}, \boldsymbol{u}) - (\boldsymbol{\sigma}_h, \boldsymbol{u}_h)\|_H^2 \;\leq\; \widetilde{C}_{\mathtt{rel}}\, \widetilde{\boldsymbol{\theta}}^2 \,.$$

The proof of Theorem 5.2 proceeds similarly as in the proof of Theorem 4.1. In fact, notice that the upper bounds for $\|\widetilde{E}_h\|_{\mathrm{H}^1_{\Gamma_{\mathrm{D}}}(\Omega)'}$ and $\|E_h\|_{\mathbb{H}_N(\mathbf{div},\Omega)'}$ given by (3.26) (*cf.* Lemma 3.6) and (4.4) (*cf.* Theorem 4.1), respectively, are also valid in 3D and hence the corresponding reliability of $\widetilde{\boldsymbol{\theta}}$ is obtained.

We end this section by remarking that the efficiency of the estimators $\boldsymbol{\theta}$ and $\widetilde{\boldsymbol{\theta}}$ follows as in Section 3.3 and Theorem 4.2, respectively. In particular, we remark that the 3D version of estimates provided in Lemmas 3.16, 3.17, and 3.18 can be derived from [22, Lemmas 4.9, 4.10, 4.11 and 4.13].

6 Numerical tests

This section serves to illustrate the properties of the estimators introduced in Sections 3-5. Fixed point iterations were used for the linearization of the coupled mixed-primal scheme, and a residual tolerance of 1e-7 was prescribed for the termination of the Picard algorithm. All linear solves are performed

with the unsymmetric multifrontal direct solver UMFPACK. In addition, all tests in this Section use a classical adaptive mesh refinement procedure based on the equi-distribution of the error indicators, where the diameter of each element in the new adapted mesh (contained in a generic element K on the initial coarse mesh) is proportional to the diameter of the initial element times the ratio $\frac{\bar{\eta}_h}{\eta_K}$, where $\bar{\eta}_h$ is the mean value of a given indicator η over the initial mesh (*cf.* [33]).

Example 1: accuracy assessment. Our first example focuses on the case where, under uniform mesh refinement, the convergence rates are affected by the singularities of the exact solutions. A non-convex domain $\Omega := (0,1)^2 \backslash [0, \frac{1}{2}]^2$ is considered, and its boundary $\partial\Omega$ is split into $\Gamma_{\rm N} := (1,0) \times \{0\}$ and $\Gamma_{\rm D} := \partial\Omega \backslash \Gamma_{\rm N}$. We construct a sequence of nested unstructured triangulations, where measured errors and experimental convergence rates will be computed as usual

$$e(\boldsymbol{\sigma}) = \|\boldsymbol{\sigma} - \boldsymbol{\sigma}_h\|_{\mathbf{div},\Omega},\ e(\phi) = \|\phi - \phi_h\|_{1,\Omega},\ e(\boldsymbol{u}) = \|\boldsymbol{u} - \boldsymbol{u}_h\|_{1,\Omega},\ r(\cdot) = -2\log(e(\cdot)/\hat{e}(\cdot))[\log(N/\hat{N})]^{-1},$$

with e and $\hat{e}$ denoting errors produced on two consecutive meshes representing N and $\hat{N}$ degrees of freedom, respectively. In addition, the total error, the modified error suggested by (3.36) and (4.5), and the effectivity and quasi-effectivity indexes associated to a given global estimator $\boldsymbol{\eta}$ are defined, respectively, as

$$\mathtt{e} = \left\{[e(\boldsymbol{\sigma})]^2 + [e(\boldsymbol{u})]^2 + [e(\phi)]^2\right\}^{1/2}, \qquad \mathtt{eff}(\boldsymbol{\eta}) = \frac{\mathtt{e}}{\boldsymbol{\eta}},$$

$$\mathtt{m} = \left\{[e(\boldsymbol{u})]^2 + [e(\phi)]^2 + \|\mathbf{div}\boldsymbol{\sigma} - \mathbf{div}\boldsymbol{\sigma}_h\|^2_{0,\Omega} + \left\|\frac{\boldsymbol{\sigma}^{\mathtt{d}}}{\mu(\phi)} - \frac{\boldsymbol{\sigma}^{\mathtt{d}}_h}{\mu(\phi_h)}\right\|^2_{0,\Omega}\right\}^{1/2}, \qquad \mathtt{qeff}(\boldsymbol{\eta}) = \frac{\mathtt{m}}{\boldsymbol{\eta}}.$$

An exact solution to (2.1) is given as follows

$$\begin{aligned}
&\phi(x_1,x_2) = m x_1 x_2 (1-x_2)(x_1-1/2)^2(x_2-1/2)^2 \ + \ b,\\
&\boldsymbol{u}(x_1,x_2) = \begin{pmatrix} \sin(\pi x_1)\cos(\pi x_2) \\ -\cos(\pi x_1)\sin(\pi x_2)\end{pmatrix}, \quad \boldsymbol{\sigma}(x_1,x_2) = \mu(\phi)\boldsymbol{u} - \left[\mu(\phi)\frac{\partial u_1}{\partial x_1} \ + \ \frac{(x_1-1)^2}{(x_2-a_1)(x_2-a_2)}\right]\mathbb{I},
\end{aligned} \tag{6.1}$$

where $\boldsymbol{K}^{-1} = K^{-1}\mathbb{I}$, $\boldsymbol{k} = (0,-1)^{\mathtt{t}}$, $\mu(\phi) = (1-a\phi)^{-2}$, $f_{\rm bk}(\phi) = a\phi(1-a\phi)^2$, $\vartheta(\phi) = \phi + (1-a\phi)^2$, and the source terms are

$$\boldsymbol{f}(x_1,x_2) = \phi^{-1}(K^{-1}\boldsymbol{u} - \mathbf{div}\boldsymbol{\sigma}), \quad g(x_1,x_2) = \beta\phi - \mathrm{div}(\vartheta(\phi)\nabla\phi) + \boldsymbol{u}\cdot\nabla\phi + f'_{\rm bk}(\phi)\boldsymbol{k}\cdot\nabla\phi.$$

Notice that the only difference with respect to (2.1) is a non-homogeneous concentration flux $\widetilde{\boldsymbol{\sigma}}\cdot\boldsymbol{\nu} = s$ imposed on $\Gamma_{\rm N}$, where s is manufactured according to (6.1). Therefore, the relevant term in the *a posteriori* error estimators will be replaced by

$$\sum_{e\in\mathcal{E}_h(T)\cap\mathcal{E}_h(\Gamma_{\rm N})} h_e\|\widetilde{\boldsymbol{\sigma}}_h\cdot\boldsymbol{\nu} - s\|^2_{0,e},$$

whose estimation from below and above follows in a straightforward way. The model parameters specifying (6.1) correspond to $m = 200$, $b = 0.008$, $a = 0.35$, $K = 0.01$, $\beta = 0.35$, and $a_1 = -0.05$, $a_2 = 1.1$. Notice that the pressure defining the isotropic part of the stress in (6.1) exhibits a singularity near the upper right corner of the domain, at (a_1, a_2) (see Fig. 6.3). As a consequence, optimal convergence for the stress is no longer evidenced under uniform mesh refinement (see first rows of Table 1). In turn, if an adaptive mesh refinement step (employing the residual error indicators $\boldsymbol{\theta}$ and $\widetilde{\boldsymbol{\theta}}$) is applied, optimal convergence can be restored, as shown in the last two blocks of Table 1. Approximated solutions obtained after six adaptation steps are collected in Figure 6.1, and a few adapted meshes produced using the two indicators are depicted in Figure 6.2. It is observed that the

D.o.f.	h	$e(\boldsymbol{\sigma})$	$r(\boldsymbol{\sigma})$	$e(\boldsymbol{u})$	$r(\boldsymbol{u})$	$e(\phi)$	$r(\phi)$	i_P	e	m	eff($\boldsymbol{\theta}$)	qeff($\boldsymbol{\theta}$)	eff($\widetilde{\boldsymbol{\theta}}$)	qeff($\widetilde{\boldsymbol{\theta}}$)
Augmented $\mathbf{RT}_0 - \mathbf{P}_1 - \mathrm{P}_1$ scheme with quasi-uniform refinement														
105	0.53	140.05	–	3.40	–	1.43	–	12	140.10	139.42	1.11	1.10	1.10	1.10
192	0.49	225.45	-6.44	8.81	-12.90	1.35	0.80	16	225.63	222.53	0.55	0.55	0.55	0.55
492	0.30	139.34	0.97	3.36	1.95	0.87	0.88	14	139.38	138.77	1.07	1.07	1.07	1.07
1488	0.16	74.51	1.01	0.82	2.27	0.47	0.98	12	74.52	74.36	0.92	0.92	0.92	0.92
4902	0.09	44.05	0.88	0.28	1.77	0.26	0.98	13	44.05	43.98	0.96	0.96	0.96	0.95
17800	0.04	21.46	1.05	0.12	1.25	0.14	0.88	13	21.46	21.43	0.98	0.98	0.98	0.98
67800	0.02	11.47	1.14	0.05	1.36	0.07	1.33	14	11.48	11.46	1.00	1.00	0.99	0.99
Augmented $\mathbf{RT}_0 - \mathbf{P}_1 - \mathrm{P}_1$ scheme with adaptive refinement according to $\boldsymbol{\theta}$														
64	0.61	203.22	–	8.93	–	1.40	–	16	203.42	197.77	0.49	0.48	–	–
171	0.35	138.78	0.77	3.07	2.17	1.18	0.34	16	138.82	138.09	1.24	1.23	–	–
303	0.33	99.71	1.15	1.98	1.52	1.10	0.26	14	99.74	99.37	0.95	0.94	–	–
499	0.30	68.36	1.51	1.27	1.78	1.09	0.03	13	68.38	68.07	1.05	1.05	–	–
1014	0.21	39.04	1.58	0.78	1.35	0.85	0.69	13	39.06	38.83	1.17	1.17	–	–
3763	0.10	16.51	1.31	0.26	1.66	0.37	1.26	13	16.52	16.45	1.07	1.07	–	–
14690	0.05	7.81	1.09	0.11	1.27	0.17	1.07	13	7.81	7.79	1.03	1.03	–	–
Augmented $\mathbf{RT}_0 - \mathbf{P}_1 - \mathrm{P}_1$ scheme with adaptive refinement according to $\widetilde{\boldsymbol{\theta}}$														
64	0.61	203.22	–	8.93	–	1.40	–	16	203.42	197.77	–	–	0.49	0.47
171	0.35	138.78	0.77	3.07	2.17	1.18	0.34	16	138.82	138.09	–	–	1.24	1.23
303	0.33	99.63	1.15	1.97	1.54	1.10	0.26	14	99.66	99.29	–	–	0.95	0.94
535	0.28	71.12	1.18	1.41	1.18	1.08	0.04	13	71.14	70.61	–	–	1.06	1.05
1145	0.21	37.86	1.65	0.60	2.24	0.80	0.79	13	37.88	37.64	–	–	1.08	1.08
4270	0.10	16.93	1.22	0.24	1.35	0.38	1.11	13	16.94	16.88	–	–	1.05	1.05
16790	0.05	8.28	1.04	0.10	1.25	0.18	1.10	13	8.28	8.26	–	–	1.02	1.01

Table 1: Test 1: convergence history, Picard iteration count, error e and quasi-error m, effectivity and quasi-effectivity indexes for the approximation of the coupled Brinkman-transport problem, under quasi-uniform, and adaptive refinement according to the indicators introduced in Sections 3 and 4.

agglomeration of points follows the regions of high concentration gradients occurring near Γ_{N}, as well as the sharp pressure profile localized at (a_1, a_2).

Example 2: sedimentation below downward-facing inclined walls. This test illustrates the properties of the second estimator (4.2) in a 2D setting, where we simulate the sedimentation of a mixture within an heterogeneous porous medium. The domain consists of an isosceles trapeze of height 3, maximal width 2.82, and walls having an angle of inclination of $4/9\pi$ with respect to the horizontal axis. The permeability of the medium is constant K_0, except for 20 randomly placed spots (consisting of disks with radii 2.5e-3) of much lower permeability K_1. Viscosity, hindering sedimentation, and compaction coefficients (all concentration-dependent) are respectively specified as

$$\mu(\phi) = \mu_0(1-\phi/\phi_{\max})^{-\eta_1}, \quad f_{\mathrm{bk}}(\phi) = u_\infty \phi(1-\phi/\phi_{\max})^{\eta_2}, \quad \vartheta(\phi) = \frac{\sigma_0 \alpha}{\phi_c^\alpha \Delta\rho G}\phi^{\alpha-2} f_{\mathrm{bk}} + u_\infty, \tag{6.2}$$

where the adimensional model parameters and remaining constants assume the values μ_0 =2.5e-4,

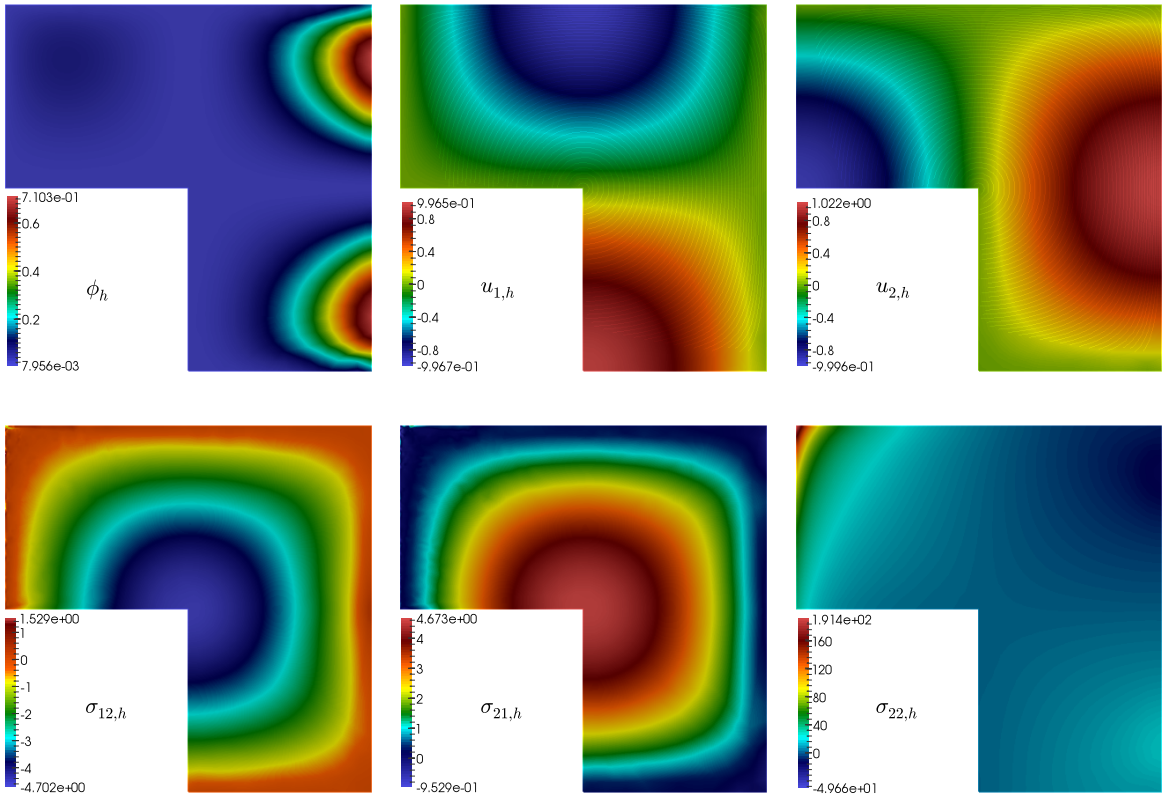

Figure 6.1: Test 1: approximate solutions obtained with the lowest order method, after six steps of adaptive mesh refinement following the second indicator $\widetilde{\boldsymbol{\theta}}$. Concentration, velocity components, and stress components are depicted.

$\sigma_0 = 5.5\text{e-}4$, $G = 9.81$, $\alpha = 5$, $\beta = 0.25$, $\eta = 2$, $\phi_c = 0.07$, $\phi_{\max} = 0.95$, $K_0 = 10$, $K_1 = 0.01$, $\boldsymbol{k} = (0, -1)^T$, $\boldsymbol{f} = (0, -1/2)^T$, $u_\infty = 2.5\text{e-}3$, $\Delta\rho = 1562$. From the physical bounds of the concentration we find $\mu_1 = \mu_0$ and $\mu_2 = 5\mu_1$, yielding the following stabilization coefficients $\kappa_1 = 1/5\mu_0^2 = 5e\text{-}5$, $\alpha_{\boldsymbol{K}} = 0.1$, $\tilde{\delta} = 4.88\text{e-}3$, $\kappa_2 = 2.38\text{e-}6$.

A pseudo time-advancing algorithm is employed to capture the transient nature of the phenomenon (this can be achieved by setting $g = \beta\phi^k$, where ϕ^k is the concentration distribution at the previous pseudo timestep). The initial guess for the concentration is a high concentration $\phi = 0.75$ on the top of the domain and a random perturbation of amplitude 0.05 around $\phi = 0.15$. We assume that the vessel is open on the top and closed elsewhere on $\partial\Omega$, so that a clear fluid $\phi = \phi_c$ and zero normal stresses $\boldsymbol{\sigma\nu} = \boldsymbol{0}$ are prescribed on top, whereas on the remainder of the boundary we set zero fluxes $\widetilde{\boldsymbol{\sigma}} \cdot \boldsymbol{\nu} = 0$ and no-slip conditions $\boldsymbol{u} = \boldsymbol{0}$.

The adaptive algorithm applies mesh refinement according to the second *a posteriori* error indicator (4.2), and it is invoked at the end of each pseudo-time step. We point out that due to the roughness of the permeability for coarser meshes, a continuation technique is applied on the viscosity scaling μ_0 (using $\tilde{\mu}_0 = 8\mu_0$ as initial guess, and halving it until reaching μ_0). A set of snapshots of the numerical solution obtained after ten pseudo-time steps are displayed in Figure 6.4. Apart from the main flow features expected in the pure-fluid case (acceleration of the deposition near the inclined walls, as discussed in [31] and simulated in [30]), we also observe tortuous concentration and velocity patterns produced by a combination of tight flow-transport coupling, the highly heterogeneous coefficients, and

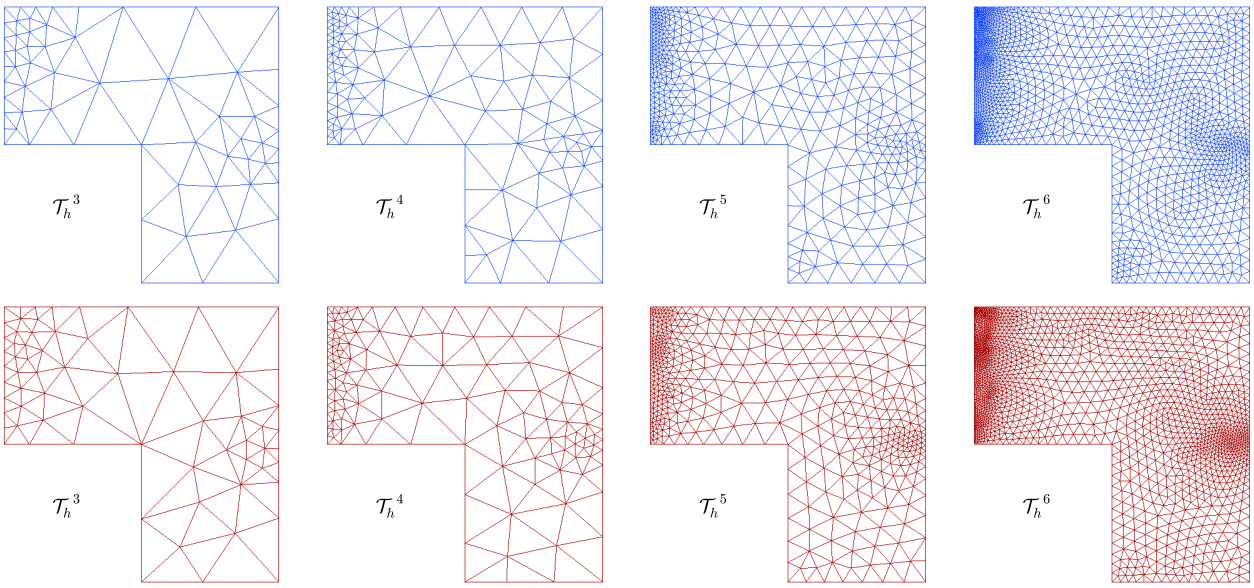

Figure 6.2: Test 1: from left to right, four snapshots of successively refined meshes according to the indicators $\boldsymbol{\theta}$ and $\widetilde{\boldsymbol{\theta}}$ (top and bottom panels, respectively).

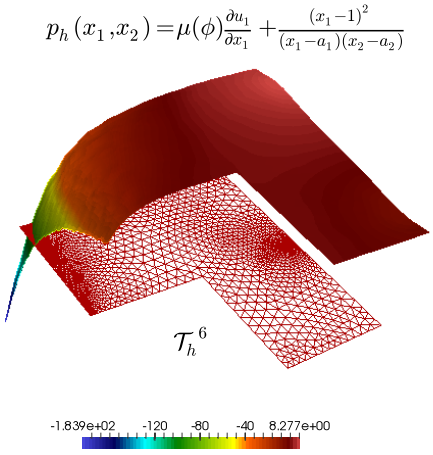

Figure 6.3: Test 1: approximate postprocessed pressure and adapted mesh near (a_1, a_2), after six refinement steps following the second estimator $\widetilde{\boldsymbol{\theta}}$.

the random initial distribution. The velocity plots (second row) indicate that the flow tends to avoid the regions of low permeability, and recirculation zones are formed near the transition from clear to high-concentration mixture. In addition, the concentration plots (panels in the first row) suggest that solid particles remain attached to the low-permeability spots and reverse plumes are formed. We also show a sequence of refined meshes after two, four, and six steps (see Figure 6.5), where it is seen that the *a posteriori* error indicator yields more refinement near the high gradients of concentration and the aforementioned recirculation zones. As these irregularities spread throughout large portions of the domain, a substantial gain in computational cost with respect to a uniformly refined mesh is not expected.

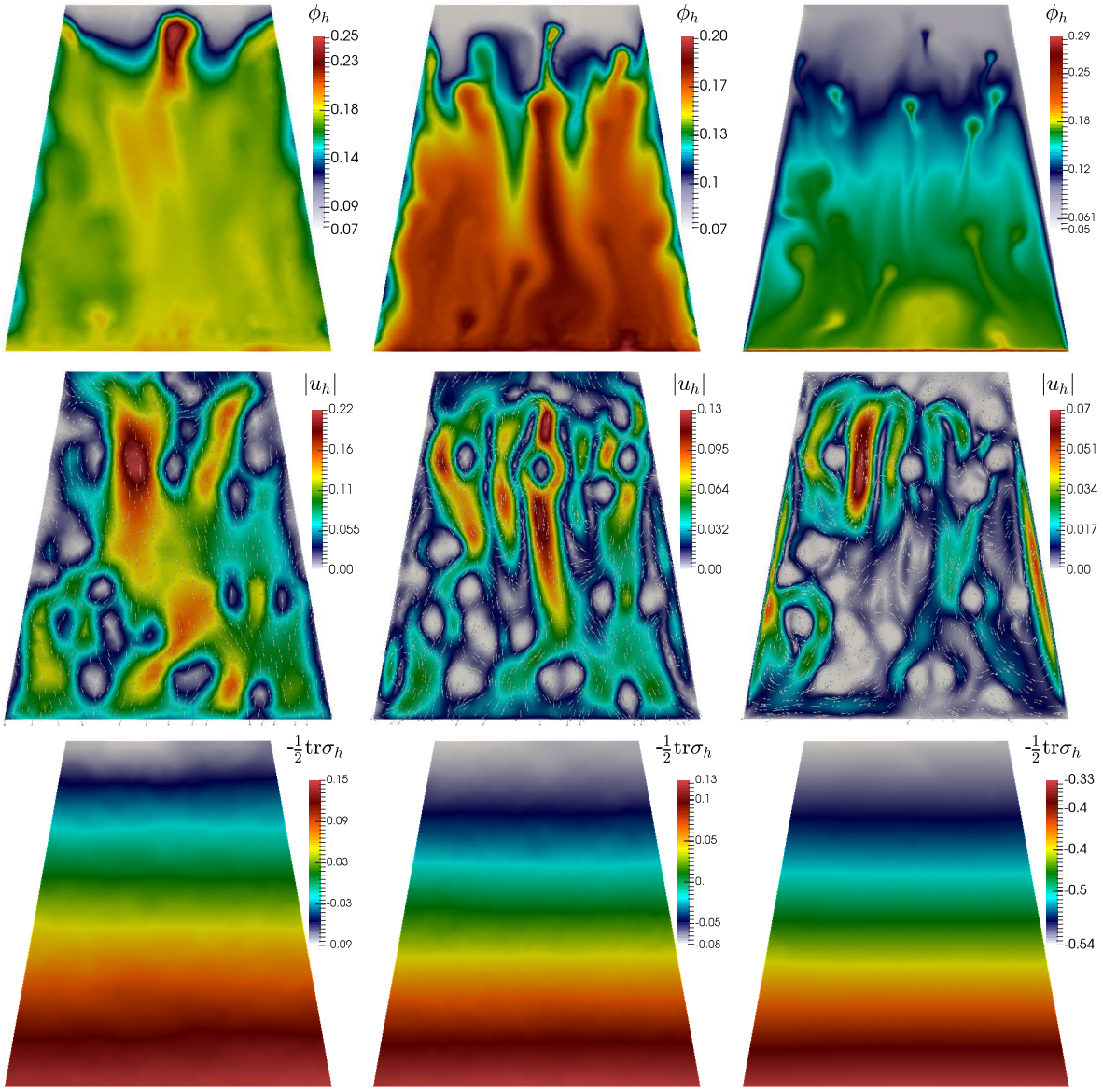

Figure 6.4: Test 2: approximate solutions at 3 (left), 6 (middle) and 12 (right) pseudo-time steps. A lowest order method and mesh adaptive refinement guided by (4.2) were used.

Example 3: sedimentation in a clarifier-thickener unit. We close this section with a numerical test that illustrates the performance of the proposed numerical scheme and the first a posteriori error indicator (5.1) on a 3D computation. The example reproduces the steady-state of a sedimentation-consolidation process in a clarifier-thickener unit. Model parameters and domain configuration are adapted from those in [5, Example 3], but here the device has a radial length of 14.6 m and a total height of 7.6 m. It features a feed inlet Γ_{in} consisting of an horizontal disk of radius 1.5 m, an underflow outlet for the discharge of sediment Γ_{out} (an horizontal disk of smaller radius 0.5 m), and a peripheral overflow annular region Γ_{ofl} (see a sketch in the top left panel of Figure 6.6). A suspension is fed through Γ_{in} with velocity $\boldsymbol{u} = \boldsymbol{u}_{\mathrm{in}} = (0, 0, -u_{3,\mathrm{in}})^T$ and having a concentration of $\phi = \phi_{\mathrm{in}}$. At the outlet Γ_{out} we set $\boldsymbol{u} = \boldsymbol{u}_{\mathrm{out}} = (0, 0, -u_{3,\mathrm{out}})^T$; at the overflow annulus we impose zero normal pseudo-stresses; and on the remainder of $\partial\Omega$ we put no slip boundary data for the velocity and zero-flux

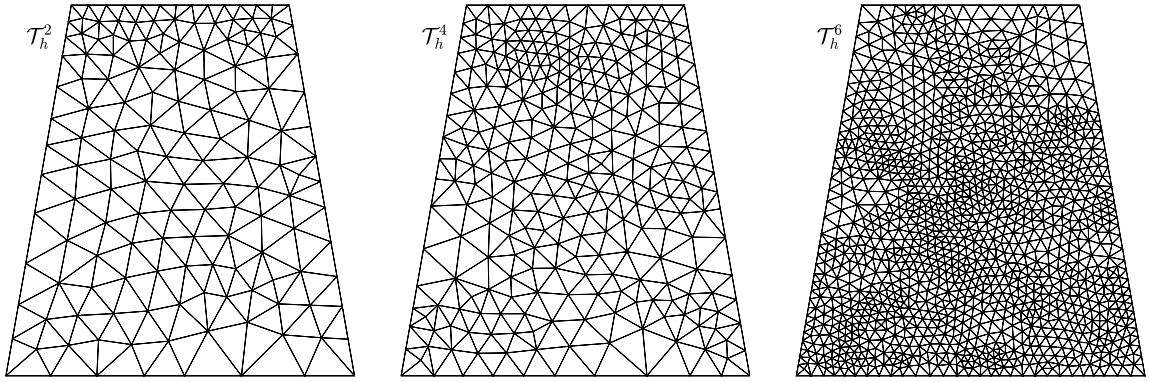

Figure 6.5: Test 2: adapted meshes at 2, 4, and 6 steps, generated following the second estimator (4.2).

conditions for the concentration.

The concentration-dependent coefficients are defined as in (6.2), and the remaining parameters are chosen as in Example 2, except for $u_{3,\text{in}}$ =1.25e-2, $u_{3,\text{out}}$ =1.25e-3, $\phi_c = 0.1$, u_∞ =2.2e-3, $\phi_{\text{in}} = 0.08$, σ_0 =5.5e-2, and β =1e-3. Again, the bounds for the concentration imply that the stabilization parameters assume the following values $\kappa_1 = 0.256$, $\kappa_2 = 0.25$.

The proposed primal-mixed method is used to generate the approximate solutions depicted in Figure 6.6 (where we show only half of the domain, for visualization purposes). As in [5, 10], we can observe that the mixture concentrates near the outlet boundary Γ_{out}. The velocity arrows show recirculating patterns, and a very small underflow. In contrast with Example 2, here the Picard iterations until convergence are embedded inside the adaptive refinement loop, consisting of solving, estimating, marking and refining using the error equi-distribution strategy mentioned above. The plots in Figure 6.7 show a sequence of three adapted meshes, forming a clustering of elements near the zones of high concentration gradients (connecting inflow and underflow boundaries), where also the velocity and postprocessed pressure profiles are more pronounced.

References

[1] R.A. Adams and J.J.F. Fournier, *Sobolev Spaces*. Academic Press. Elsevier Ltd, 2003.

[2] C. Amrouche, C. Bernardi, M. Dauge, and V. Girault, *Vector potentials in tree-dimensional nonsmooth domains*. Math. Methods. Appl. Sci., 21 (1998) 823–864.

[3] M. Alvarez, G.N. Gatica and R. Ruiz-Baier, *A mixed-primal finite element approximation of a sedimentation-consolidation system*. M3AS: Math. Models Methods Appl. Sci., 26 (2016), no. 5, 867–900.

[4] M. Alvarez, G.N. Gatica and R. Ruiz-Baier, *A posteriori error analysis for a viscous flow-transport problem*. ESAIM: Math. Model. Numer. Anal., DOI: http://dx.doi.org/10.1051/m2an/2016007.

[5] M. Alvarez, G.N. Gatica and R. Ruiz-Baier, *An augmented mixed–primal finite element method for a coupled flow–transport problem*. ESAIM: Math. Model. Numer. Anal. 49 (2015), no. 5, 1399–1427.

[6] I. Babuška and G.N. Gatica, *A residual-based a posteriori error estimator for the Stoke-Darcy coupled problem*. SIAM J. Numer. Anal. 48 (2010), no. 2, 498–523.

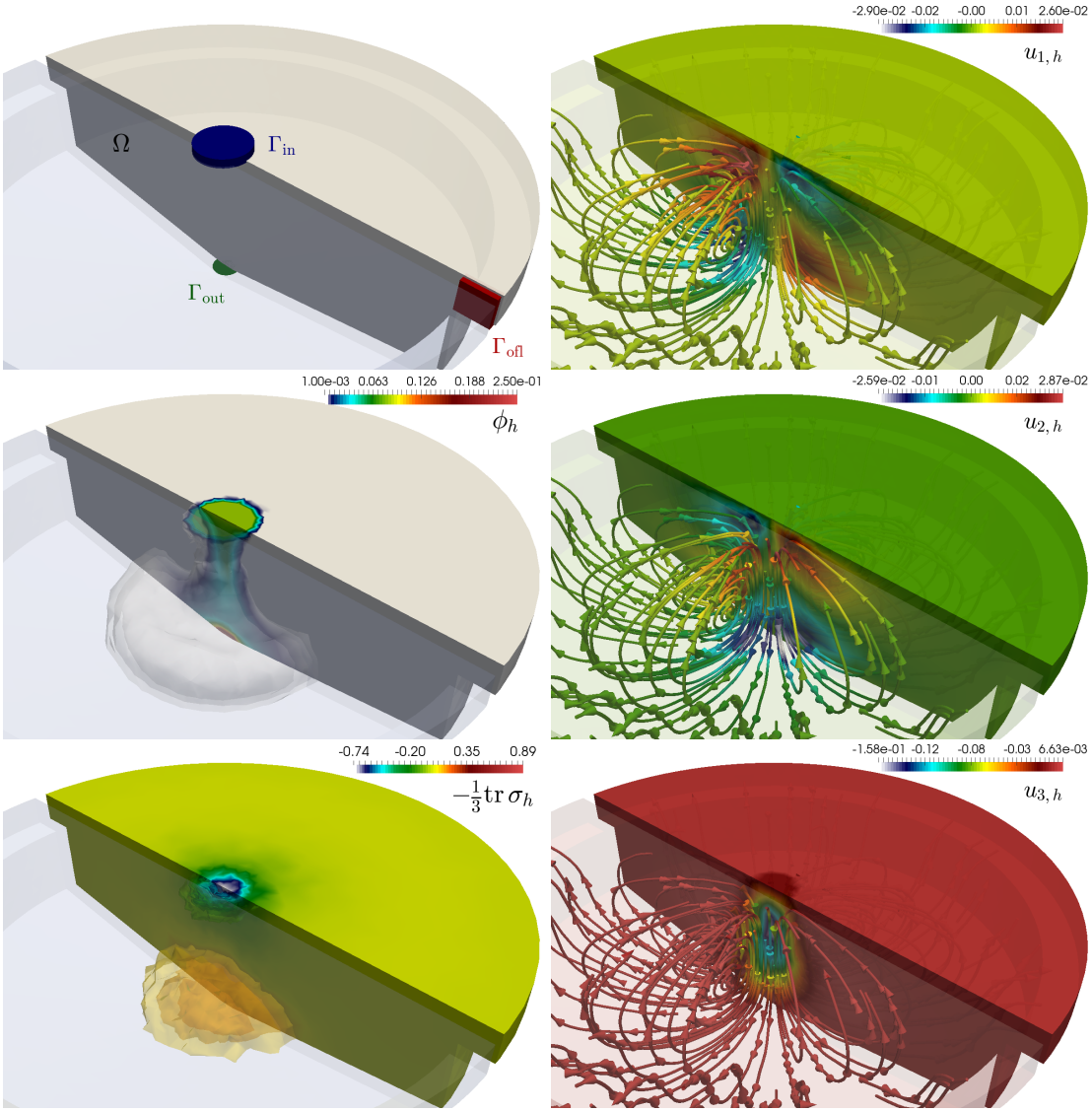

Figure 6.6: Test 3: sketch of the clipped domain and different boundaries in a clarifier-thickener device (top left panel), and snapshots of the approximate concentration, postprocessed pressure, and velocity components and streamlines computed with the proposed lowest order mixed-primal method.

[7] C. Bernardi, L. El Alaoui, and Z. Mghazli, *A posteriori analysis of a space and time discretization of a nonlinear model for the flow in partially saturated porous media*. IMA J. Numer. Anal. 34 (2014), no. 3, 1002–1036.

[8] M. Braack and T. Richter, *Solving multidimensional reactive flow problems with adaptive finite elements*. Reactive flows, diffusion and transport, 93–112, Springer, Berlin, 2007.

[9] F. Brezzi and M. Fortin, *Mixed and Hybrid Finite Element Methods*. Springer-Verlag, 1991.

[10] R. Bürger, R. Ruiz-Baier and H. Torres, *A stabilized finite volume element formulation for sedimentation-consolidation processes*. SIAM J. Sci. Comput. 34 (2012), no. 3, B265–B289.

[11] C. Carstensen, *A posteriori error estimate for the mixed finite element method*. Mathematics of Computation, 66 (1997), no. 218, 465–476.

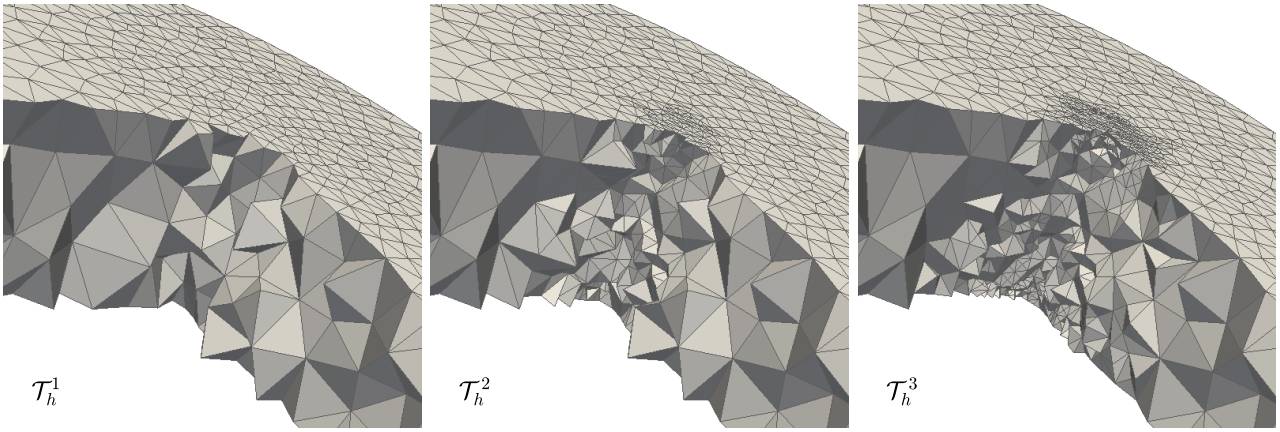

Figure 6.7: Test 3: zoom on the produced meshes after the first three steps of adaptive refinement using the first estimator as defined in (5.1).

[12] C. Carstensen and G. Dolzmann, *A posteriori error estimates for mixed FEM in elasticity.* Numerische Mathematik, 81 (1998), no. 2, 187–209.

[13] P. Ciarlet, *The Finite Element Method for Elliptic Problems.* North-Holland, 1978.

[14] P. Clément, *Approximation by finite element functions using local regularization.* RAIRO Model, Math. et Anal. Numer. 9 (1975), no. 2, 77–84.

[15] D.A. Di Pietro, E. Flauraud, M. Vohralík, and S. Yousef, *A posteriori error estimates, stopping criteria, and adaptivity for multiphase compositional Darcy flows in porous media.* J. Comput. Phys. 276 (2014), 163–187.

[16] C. Domínguez, G.N. Gatica and S. Medahi, *A posteriori error analysis of a fully-mixed finite element method for a two-dimensional fluid-solid interaction problem.* J. Comput. Math. 33 (2015), no. 6, 606-641.

[17] A.I. Garralda-Guillen, G.N. Gatica, A. Márquez and M. Ruiz, *A posteriori error analysis of twofold saddle point variational formulations for nonlinear boundary value problems.* IMA Journal of Numerical Analysis, 34 (2014), no. 1, 326–361.

[18] G.N. Gatica, *A note on the efficiency of residual-based a-posteriori error estimators for some mixed finite element methods.* Elec. Trans. Numer. Anal. 17 (2004), 218–233.

[19] G.N. Gatica, *A Simple Introduction to the Mixed Finite Element Method: Theory and Applications.* Springer Briefs in Mathematics. Springer, Cham, 2014.

[20] G.N. Gatica, *A note on stable Helmholtz decompositions in 3D.* Preprint 2016-03, Centro de Investigación en Ingeniería Matemática (CI^{2}MA). Universidad de Concepción, Chile, (2016). [available from `http://www.ci2ma.udec.cl`].

[21] G.N. Gatica, L.F. Gatica and A. Márquez, *Analysis of a pseudostress-based mixed finite element method for the Brinkman model of porous media flow.* Numer. Math. 126 (2014), no. 4, 635–677.

[22] G.N. Gatica, L.F. Gatica, and F.A. Sequeira, *A priori and a posteriori error analyses of a pseudostress-based mixed formulation for linear elasticity.* Comput. Math. Appl. 71 (2016), no. 2, 585-614.

[23] G.N. Gatica, A. Márquez and M.A. Sánchez, *Analysis of a velocity-pressure-pseudostress formulation for the stationary Stokes equations.* Comput. Methods Appl. Mech. Engrg. 199 (2010), no. 17-20, 1064–1079.

[24] G.N. Gatica, A. Márquez and M.A. Sanchez, *A priori and a posteriori error analysis of a velocity-pseudostress formulation for a class of quasi-Newtonian Stokes flows*. Comput. Methods Appl. Mech. Engrg. 200 (2011), no. 17-20, 1619–1636.

[25] V. Girault, and P. A. Raviart, *Finite element methods for Navier-Stokes equations. Theory and algorithms*. Springer-Verlag, Berlin, 1986.

[26] M.G. Larson and A. Målqvist, *Goal oriented adaptivity for coupled flow and transport problems with applications in oil reservoir simulations*. Computs. Methods Appl. Mech. Engrg. 196 (2007), no. 37-40, 3546–3561.

[27] M.G. Larson, R. Söderlund and F. Bengzon, *Adaptive finite element approximation of coupled flow and transport problems with applications in heat transfer*. Int. J. Numer. Meth. Fluids. 57 (2008), no. 9, 1397–1420.

[28] A. Quarteroni and A. Valli, *Numerical Approximation of Partial Differential Equations*. Springer Series in Computational Mathematics, vol. 23, Springer-Verlag Berlin Heidelberg 1994.

[29] J.E. Roberts and J.M. Thomas, *Mixed and Hybrid Methods*. In Handbook of Numerical Analysis, edited by P.G. Ciarlet and J.L Lions, vol. II, Finite Elements Methods (Part 1), Nort-Holland, Amsterdam, 1991.

[30] R. Ruiz-Baier and H. Torres, *Numerical solution of a multidimensional sedimentation problem using finite volume-element methods*. Appl. Numer. Math. 95 (2015), no. 1, 280–291.

[31] U. Schaflinger, *Experiments on sedimentation beneath downward-facing inclined walls*, Int. J. Multiphase Flow 11 (1985), no. 1, 189–199.

[32] S. Sun and M.F. Wheeler, *Local problem-based a posteriori error estimators for discontinuous Galerkin approximations of reactive transport*. Comput. Geosci. 11 (2007), no. 2, 87–101.

[33] R. Verfürth, *A posteriori error estimation and adaptive-mesh-refinement techniques*. J. Comput. Appl. Math. 50 (1994), no. 1-3, 67–83.

[34] R. Verfürth, *A Review of A Posteriori Error Estimation and Adaptive-Mesh-Refinement Techniques*. Wiley-Teubner (Chichester), 1996.

[35] M. Vohralík and M.F. Wheeler, *A posteriori error estimates, stopping criteria, and adaptivity for two-phase flows*. Comput. Geosci. 17 (2013), no. 5, 789–812.

Centro de Investigación en Ingeniería Matemática (CI^{2}MA)

PRE-PUBLICACIONES 2016

2016-15 Rodolfo Araya, Christopher Harder, Abner Poza, Frederic Valentin: *Multiscale hybrid-mixed method for the Stokes and Brinkman equations - The method*

2016-16 Luis M. Castro, José González, Víctor H. Lachos, Alexandre Patriota: *A confidence set analysis for observed samples: A fuzzy set approach*

2016-17 Raimund Bürger, Stefan Diehl, Camilo Mejías: *A model of continuous sedimentation with compression and reactions*

2016-18 Carlos Garcia, Gabriel N. Gatica, Salim Meddahi: *Finite element analysis of a pressure-stress formulation for the time-domain fluid-structure interaction problem*

2016-19 Anahi Gajardo, Benjamin Hellouin, Diego Maldonado, Andres Moreira: *Nontrivial turmites are Turing-universal*

2016-20 Leonardo E. Figueroa: *Error in Sobolev norms of orthogonal projection onto polynomials in the unit ball*

2016-21 Raimund Bürger, Julio Careaga, Stefan Diehl: *Entropy solutions of a scalar conservation law modelling sedimentation in vessels with varying cross-sectional area*

2016-22 Akhlesh Lakhtakia, Peter Monk, Cinthya Rivas, Rodolfo Rodríguez, Manuel Solano: *Asymptotic model for finite-element calculations of diffraction by shallow metallic surface-relief gratings*

2016-23 Sergio Caucao, Gabriel N. Gatica, Ricardo Oyarzúa: *A posteriori error analysis of a fully-mixed formulation for the Navier-Stokes/Darcy coupled problem with nonlinear viscosity*

2016-24 Jessika Camaño, Gabriel N. Gatica, Ricardo Oyarzúa, Ricardo Ruiz-Baier: *An augmented stress-based mixed finite element method for the Navier-Stokes equations with nonlinear viscosity*

2016-25 Jessika Camaño, Luis F. Gatica, Ricardo Oyarzúa: *A priori and a posteriori error analyses of a flux-based mixed-FEM for convection-diffusion-reaction problems*

2016-26 Mario Álvarez, Gabriel N. Gatica, Ricardo Ruiz-Baier: *A posteriori error analysis for a sedimentation-consolidation system*

Para obtener copias de las Pre-Publicaciones, escribir o llamar a: Director, Centro de Investigación en Ingeniería Matemática, Universidad de Concepción, Casilla 160-C, Concepción, Chile, Tel.: 41-2661324, o bien, visitar la página web del centro: `http://www.ci2ma.udec.cl`







Centro de Investigación en
Ingeniería Matemática (CI²MA)
Universidad de Concepción

Casilla 160-C, Concepción, Chile
Tel.: 56-41-2661324/2661554/2661316
http://www.ci2ma.udec.cl